

12-2019

## Incorporating Geophysical Data in Slope Stability Modeling for Two Slopes in Arkansas

Vanessa LeBow  
*University of Arkansas, Fayetteville*

Follow this and additional works at: <https://scholarworks.uark.edu/etd>



Part of the [Civil Engineering Commons](#), [Geophysics and Seismology Commons](#), [Geotechnical Engineering Commons](#), and the [Structural Engineering Commons](#)

---

### Citation

LeBow, V. (2019). Incorporating Geophysical Data in Slope Stability Modeling for Two Slopes in Arkansas. *Theses and Dissertations* Retrieved from <https://scholarworks.uark.edu/etd/3492>

This Thesis is brought to you for free and open access by ScholarWorks@UARK. It has been accepted for inclusion in Theses and Dissertations by an authorized administrator of ScholarWorks@UARK. For more information, please contact [ccmiddle@uark.edu](mailto:ccmiddle@uark.edu).

Incorporating Geophysical Data in Slope Stability  
Modeling for Two Slopes in Arkansas

A thesis submitted in partial fulfillment  
of the requirements for the degree of  
Master of Science in Civil Engineering

by

Vanessa LeBow  
University of Arkansas  
Bachelor of Science in Civil Engineering, 2018

December 2019  
University of Arkansas

This thesis is approved for the recommendation to the Graduate Council.

---

Michelle Barry, Ph.D.  
Thesis Chair

---

Norman Dennis, Ph.D.  
Committee member

---

Clinton Wood, Ph.D.  
Committee member

## **Abstract**

Slope failures in the United States alone cause millions of dollars in damage to infrastructure, threaten national monuments, create environmental hazards, and take an average of 25-50 lives a year. With the inevitable construction that occurs on slopes, it is imperative that the slopes be properly designed which requires a thorough understanding of slope grade, subsurface soil conditions, soil strength parameters, water table locations, and depth to bedrock across the entire site. The preferred method of data collection would be to use borings and other in-situ methods; however, sometimes due to cost constraints or site accessibility only a very limited number of borings can be taken at a site. Another option, is to use geophysical methods of data collection. These techniques are non-destructive, efficient, cost-effective for large areas, and have been shown to be reliable in past studies. This paper investigated how the addition of geophysical data affects the slope stability analysis for two slopes located in Arkansas. One slope was located in Sand Gap, Arkansas and the second slope was located in Ozark, Arkansas. Slide by Rocscience was used as the stability software and the Simplified Bishop, Simplified Janbu, and Morgenstern-Price were selected as the methods of analysis. The results from this study show that the addition of geophysical data can greatly impact the calculated factor of safety for a slope as well as the failure locations, especially at sites where a very limited number of borings were taken.

## **Acknowledgments**

First and foremost, I would like to give thanks to God above for allowing me the opportunity to pursue a master's degree in the field that I love. I pray that I can use the knowledge I have gained to bring more glory to Him and to leave the world a better place than when I arrived. Second, I would like to extend thanks to the amazing faculty in the University of Arkansas Civil Engineering program. In my time here, I have seen many of them go above and beyond to help the students in this program succeed. Most specifically, I would like to give thanks to my wonderful advisor, Dr. Michelle Barry. She has been an integral part of my success throughout my undergraduate and graduate career. From reviewing my papers and writing letters of recommendation to giving life advice and talking home improvement techniques, Dr. Barry has made a personal investment in not only my success as a student, but as a person, and for that I am truly grateful. I would also like to thank Dr. Clinton Wood and Dr. Norman Dennis for providing guidance during my research process as well as volunteering to be members of my committee. Lastly, I would like to thank my amazing family. While they were rarely interested in my research and study topics, they never hesitated to encourage me and remind of me how proud they were of me. Most specifically my husband Caleb, who has been my biggest fan and supporter throughout my time in graduate school. He has been my best friend and in times of doubt reminded me that I can do anything that I set my mind to and am willing to work for. Caleb, thank you and I love you.

## **Table of Contents**

Introduction.....	1
Limit Equilibrium.....	2
Numerical Analysis.....	4
2D and 3D Analysis.....	5
Geophysics.....	5
ERT.....	6
HVSr.....	7
MASW.....	7
Past Studies.....	8
Methodology.....	10
Site Backgrounds.....	10
Analysis Methods.....	15
Sand Gap Site Analysis.....	16
Ozark Site Analysis.....	22
Results and Discussion.....	28
Sand Gap Site.....	28
Perpendicular Line.....	28
High Low Line.....	40
Ozark Site.....	46
Line 1.....	46
Line 2.....	61
Conclusion.....	73
References.....	75

## **List of Figures**

Figure 1 Typical MASW Setup.....	8
Figure 2 Sand Gap Testing Area.....	10
Figure 3 Longitudinal Crack Located on Highway 7.....	11
Figure 4 Testing Locations for Sand Gap.....	12
Figure 5 Testing Area for Ozark Site.....	13
Figure 6 Longitudinal Pavement Cracking and Soil Cracking.....	13
Figure 7 Testing Locations for Borings and Geophysics for Ozark.....	14
Figure 8 Cross-sections Taken for Slope Models.....	17
Figure 9 Models used for Phase 1 Slope Analysis for (a) Perpendicular Line and (b) High Low Line Cross-sections.....	19
Figure 10 Models used for Phase 2 Slope Analysis for (a) Perpendicular Line and (b) High Low Line Cross-sections.....	21
Figure 11 Slope Cross-sections for Ozark Site.....	22
Figure 12 Models used for Phase 2 Slope Analysis for (a) Perpendicular and (b) High Low Line Cross-sections.....	25
Figure 13 Models used for Phases 2-4 Slope Analysis for (a) Perpendicular and (b) High Low Line Cross Sections.....	27
Figure 14 Parametric Study for Phase 1 Perpendicular Line using (a) Simplified Bishop, (b) Simplified Janbu, and (c) Morgenstern-Price Method.....	29
Figure 15 ERT Line 1 and MASW Line 1 Bedrock Line with Borings overlaid.....	31
Figure 16 Parametric Study for Phase 2 Perpendicular Line using (a) Simplified Bishop, (b) Simplified Janbu, and (b) Morgenstern-Price Method.....	33
Figure 17 Parametric Study Zoomed in for Phase 2 Perpendicular Line using (a) Simplified Bishop, (b) Simplified Janbu, and (b) Morgenstern-Price Method.....	35
Figure 18- Parametric Study for Phase with Weak Layer Perpendicular Line using (a) Simplified Bishop, (b) Simplified Janbu, (c) Morgenstern-Price Method.....	37
Figure 19 Parametric Study Zoomed in for Phase 2 after addition of Weak Layer Perpendicular Line using (a) Simplified Bishop, (b) Simplified Janbu, (c) Morgenstern-Price Method.....	38
Figure 20 (a) Parametric Study for Phase 1 High Low Line using (a) Simplified Bishop, (b) Simplified Janbu, and (c) Morgenstern-Price Method.....	42

Figure 21 Parametric Study for Phase 2 High Low Line using (a) Simplified Bishop, (b) Simplified Janbu, (c) Morgenstern-Price Method.....	44
Figure 22 Parametric Study for Phase 1 Line 1 using (a) Simplified Bishop, (b) Simplified Janbu, (c) Morgenstern-Price Method.....	47
Figure 23 Ozark Site (a) ERT Line 1, (b) ERT Line 3, (c) ERT Line 8.....	49
Figure 24 Ozark Site (a) MASW Line 1, (b) MASW Line 3, (c) MASW Line 8.....	51
Figure 25 Parametric Study for Phase 2 Line 1 using (a) Simplified Bishop, (b) Simplified Janbu, (c) Morgenstern-Price Method.....	53
Figure 26 Parametric Study for Phase 3 Line 1 using (a) Simplified Bishop, (b) Simplified Janbu, (c) Morgenstern-Price Method.....	55
Figure 27 Parametric Study for Phase 4 Part 1 Line 1 using (a) Simplified Bishop, (b) Simplified Janbu, (c) Morgenstern-Price Method.....	57
Figure 28 Parametric Study for Phase 4 Part 2 Line 1 using (a) Simplified Bishop, (b) Simplified Janbu, (c) Morgenstern-Price Method.....	59
Figure 29 Parametric Study for Phase 1 Line 2 using (a) Simplified Bishop, (b) Simplified Janbu, (c) Morgenstern-Price Method.....	63
Figure 30 Parametric Study for Phase 2 Line 2 using (a) Simplified Bishop, (b) Simplified Janbu, (c) Morgenstern-Price Method.....	65
Figure 31 Parametric Study for Phase 3 Line 2 using (a) Simplified Bishop, (b) Simplified Janbu, (c) Morgenstern-Price Method.....	67
Figure 32 Parametric Study for Phase 4 Part 1 Line 2 using (a) Simplified Bishop, (b) Simplified Janbu, (c) Morgenstern-Price Method.....	69
Figure 33 Parametric Study for Phase 4 Part 2 Line 2 using (a) Simplified Bishop, (b) Simplified Janbu, (c) Morgenstern-Price Method.....	71

## **List of Tables**

Table 1: Factors that Decrease Shear Strength and Increase Shear Stress.....	1
Table 2: Recommended Minimum Values of FOS.....	2
Table 3: SPT to Friction Angle Correlations.....	15
Table 4: SPT to Unit Weight Correlations.....	16
Table 5: Soil Description Classification based on Soil Strength.....	16
Table 6: Bedrock Classification based on Rock Quality Density.....	16
Table 7: Soil Strength Parameters for the Sand Gap Site.....	18
Table 8: Soil Strength Parameters for the Ozark Site.....	24
Table 9: FOS Tabulations for Sand Gap Site Perpendicular Line.....	40
Table 10: FOS Tabulations for Sand Gap Site High Low Line.....	45
Table 11: FOS Tabulations for Ozark Site Line 1.....	61
Table 12: FOS Tabulations for Ozark Site Line 2.....	73



## **Introduction**

Slope failures in the United States alone cause millions of dollars in damage to infrastructure every year (Schuster, 1996). They additionally create environmental hazards, threaten national monuments (Toastti, 2008), and take an average of 25-50 lives each year in the United States alone (USGS, 2018). Finding a way to better understand slopes can improve slope design and in turn save money and lives. Duncan and Wright (2005) identified the two causes of slope failure as 1) a decrease in the soil's shear strength and 2) an increase in the stress that the soil feels. Table 1 presents a breakdown of the main factors that can lead to an unstable slope.

Table 1: Factors that Decrease Shear Strength and Increase Shear Stress (Duncan and Wright, 2005)

Decreases Shear Strength:	Increases Shear Stress:
1) Increased pore pressure	1) Loads at the top of the slope
2) Soil cracking	2) Water pressure in cracks at the top of the slope
3) Swelling in clays	3) Increase in soil weight due to increased water content
4) Development of slickensides	4) Excavation at the bottom of the slope
5) Decomposition of clayey rock fills	5) Drop in water level at the base of the slope
6) Creep under sustained loads	6) Earthquake shaking
7) Leaching	
8) Brittle soils undergoing strain softening	
9) Weathering	
10) Cyclic loading	

It should be noted that it is impossible to isolate a single variable as the cause of slope instability. Typically, multiple factors contribute to the actual cause of the slope failure (Sowers, 1979). The key to preventing a slope failure, as well as, rehabilitating a failed slope is to identify the causes and location of the failure which can be achieved through the use of slope stability software and field investigations. Slope stability software is used to find the minimum factor of

safety (FOS), which is defined as the available shear strength,  $s$ , divided by the equilibrium shear stress,  $\tau$ , shown in Equation 1.

$$FOS = s / \tau \quad \text{Equation 1}$$

The larger the FOS, the more stable or safer the slope is deemed to be. A FOS equal to or less than 1.0 is considered unstable. The recommended FOSs typically used in design are displayed in Table 2.

Table 2: Recommended Minimum Values of FOS (Duncan and Wright, 2005)

	Uncertainty of analysis conditions	
	Small	Large
Cost and consequences of slope failure		
Cost of repair comparable to incremental cost to construct more conservatively designed slope	1.25	1.5
Cost of repair much greater than incremental cost to construct more conservatively designed slope	1.5	2.0 or greater

The typical FOS used for low risk slopes is 1.3 (Stark and Ruffing, 2017). The two main methods for calculating how safe a slope is in a slope stability analysis are limit equilibrium and numerical analysis; however, it should be noted that artificial neural networks and limit analysis are also viable methods (Pourkhosravani and Kalantari, 2011).

### **Limit Equilibrium**

Limit equilibrium methods have been in use for decades and have been shown to be reliable in slope stability assessments. It has also been shown that limit equilibrium methods are preferred when the site has limited data (Matthews et al., 2014) and when the site has a low FOS and reinforcement is to be added (Moudabel, 1997). The limit equilibrium method uses Mohr-Coulomb criteria and the principles of static equilibrium to find the FOS. The goal is to satisfy

the following three static equilibrium conditions: 1) moment equilibrium about any point, 2) equilibrium of forces in the horizontal direction, and 3) equilibrium of forces in the vertical directions. Each scenario begins as a statically indeterminate problem, and thru assumptions becomes a statically determinate problem that can be solved (Duncan and Wright, 2005). To find the surface that is most at risk of failing, the limit equilibrium methods test numerous different potential sliding masses, and respective failure surfaces, to find the one with the lowest FOS, which is the surface that is likely to govern the slope's behavior (Leschinsky and Ambauen, 2015). There are two general approaches taken when employing limit equilibrium. The first is to calculate equilibrium over the entire sliding mass, known as the single free-body procedure. The second, and more common approach, divides the sliding mass into slices and calculates equilibrium about each slice. This approach is known as the method of slices. There are many different methods that fall into the method of slices category and each make different assumptions to create statically indeterminate problems (Duncan and Wright, 2005). For this study, Simplified Bishop (Bishop, 1955), Simplified Janbu (Janbu, 1973), and Morgenstern-Price (Morgenstern-Price, 1965) methods were selected and are further discussed here.

Simplified Bishop method assumes a circular failure surface and that the shear forces between slices are horizontal, which means that there are no shear forces. Moment equilibrium about the center of the circle and equilibrium of the vertical forces are satisfied; however, equilibrium of the forces acting horizontally are not (Bishop, 1955). While this method is one of the more simple methods and confined to circular failure planes, Wright et al. (1973) showed that when compared to other more complicated limit equilibrium methods, Simplified Bishop calculated a FOS that was within 5% of the FOSs calculated by the other methods.

Simplified Janbu is considered a Force Equilibrium method, meaning that the static equilibrium conditions for forces in the vertical and horizontal directions are met. This is done by assuming the inclination of the forces so that they can be calculated. Typically, the Simplified Janbu Method gives a very conservative (low) FOS; however a correction factor is applied to produce a more realistic FOS (Janbu et al., 1956; Janbu, 1973).

Lastly, Morgenstern-Price is a Complete Equilibrium Procedure that assumes that a relationship exists between the shear and normal forces and that the normal force acts at the center of the slice at the base. These assumptions allows all three static equilibrium conditions to be met (Morgenstern-Price, 1965).

### **Numerical Analysis**

Numerical analysis methods use a more sophisticated and complicated approach to slope stability problems. Rather than giving an exact solution to the governing equations, numerical analysis methods use reasonable approximations, or analytical solutions. Additionally, these methods take deformation and strain, into account as well as forces and stresses. Numerical analysis methods can be broadly subdivided into two categories, continuum and discontinuum. Finite Difference Method (FDM) and Finite Element Method (FEM) are the two most common continuum methods and Distinct Element Methods (DEM) and Discontinuous Deformation Analysis (DDA) are the most common Discontinuum methods (Leschinsky and Ambauen, 2015). While these methods are considered to be more accurate, they are also time consuming and rigorous (Lin et.al, 2014). For this study, limit equilibrium methods will be used due to the fact that both sites had relatively limited data and the Ozark site had anchors installed in the slope.

## **2D and 3D Analysis**

Slope stability analysis can be conducted using either 2D or 3D methods, each having pros and cons. The most widely used method is 2D stability analyses that assume plane strain conditions. 2D slope models are favored due to their relatively simple model creation, quick simulation times, and generally conservative results; however, 2D software does have some downfalls. In some cases 2D problems lack the ability to properly represent the true nature of the problem and can yield unrealistic results (Wines, 2016). It should also be noted that 2D simulations generally produce a lower FOS than a 3D simulation (Albatineh, 2006). 3D analyses are believed to better encompass the full nature of a slope and, therefore, the results are generally considered to be more accurate. The negatives of 3D modeling software include increased model creation complexity, increased simulation time, and increased costs for software purchase. Due to these reasons, 2D analysis was selected for this study.

## **Geophysics**

Selecting the slope stability analysis method is important, however the accuracy of the analysis relies heavily on the input data. Ideal input data requires a thorough understanding of the slope's subsurface conditions including soil types, layer thicknesses, soil strength parameters, soil unit weights, location of the water table, and relative elevations along the slope. The absence of any of these parameters decreases the accuracy and reliability of the model. Traditionally, the most popular method for collecting subsurface information has been through drilling and sampling. Boring logs provide accurate data for selected points along a slope, however, they do not provide any information about the soil profile between boring locations. This decreases an engineer's understanding of the overall slope stratigraphy and increases the chance of making unconservative, or even overly conservative, interpretations between the borings. Adding

additional borings can be expensive, invasive, and even unpractical due to accessibility issues or slope steepness. Another option is to use geophysical, or noninvasive, techniques which have several advantages. Geophysical methods are non-destructive and they are more efficient and cost-effective for larger areas compared to drilling or excavation. Additionally, these techniques have been used and improved upon for more than half a century making them increasingly more reliable (Everett, 2014; EEGS, 2018). It should be noted however that using geophysical data does have some negatives. Jongmans and S. Garambois (2007) discussed the following three drawbacks of geophysics: 1) the resolution decreases with depth, 2) the data produces a non-unique solution which may require calibration, and 3) results generally produce indirect subsoil information rather than geotechnical properties. Pazzi et al. (2019) states that even though geophysical methods have limitations, they can generally be overcome when used in conjunction with drilling and other geotechnical practices. Some of the most common geophysical methods include electrical resistivity tomography (ERT), capacitively-coupled resistivity (CCR), horizontal-to-vertical spectral ratio (HVSr), multichannel analysis of surface waves (MASW), seismic refraction, and ground penetrating radar (GPR). This study employs the use ERT, HVSr, and MASW testing. A brief introduction to each is given here.

### ***ERT***

One means of collecting geophysical data is through electrical resistivity tomography (ERT). For this process, a multi-electrode resistivity meter is used to measure subsurface resistivity. Resistivity represents the resistance to, or the difficulty of passing an electrical current through a material and can be measured using either direct current or alternating current. The differences in resistivity allow engineers and geologists to find profile properties such as soil interfaces and the presence of water, when electrical contrasts are present. However, it is noted

that a single material can have a range of resistivity values based on concentration of ions, weathering, level of saturation, etc. ERT interpretations when supported by other data can offer an accurate representation of the subsurface soil profile and geologic formations (Everett, 2014; Zhou, 2018). ERT methods are one of the most common geophysical methods used in slope stability analysis (Pazzi, 2019).

### ***HVSR***

Horizontal-to-vertical spectral ratio (HVSR) is a passive form of collecting geophysical data, meaning that it does not require an artificial source to create a subsurface seismic response. Instead, this method relies on microtremors and ambient noise produced by natural or manmade sources such as wind, ocean waves, or traffic. Using a broad-band three component seismic sensor, the microtremors are recorded and the horizontal-to-vertical frequency spectrum is estimated used to calculate the fundamental site resonance frequency, which in turn can be used to estimate sediment thickness and bedrock depth (Lane et al. 2008). HVSR falls into the category of micro seismic noise (SN), which is a common method used in slope stability analysis. It tends to be more commonly used in rock stability issues, but has also been used in several studies involving soil instability (Pazzi et al., 2019).

### ***MASW***

Multichannel analysis of surface waves (MASW) is another form of geophysical data collection where the stiffness, or elastic conditions, of the ground are evaluated. An impact, such as a sledge hammer hitting a metal plate, is used to create seismic surface waves that travel through the material underground. The velocities of these waves are measured using evenly spaced geophones. Figure 1 below shows a typical MASW setup.

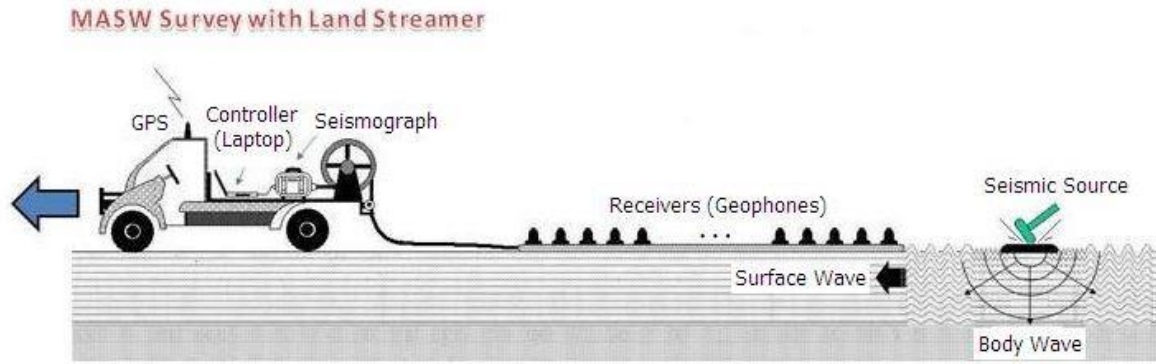


Figure 1- Typical MASW Setup (Retrieved from <http://www.masw.com/DataAcquisition.html>)

The surface wave velocities are recorded and used to find shear wave velocities, which is an elastic constant. Additionally, shear wave velocity can be related back to young's modulus and in turn be correlated to material strength. Therefore, MASW can be used not only to provide the geometry of the soil profile, but also the stiffness of the soils (Park et al., 1999). MASW methods have not been a common tool for slope stability investigations, but are becoming increasingly more popular according to Pazzi et al (2019).

### Past Studies

Since the 1970's geophysicists, geologists and engineers have been using different types of geophysical methods in slope stability analysis, the most common being ERT, SN, and seismic refraction (SR). Pazzi et al. (2019) showed that in studies where geophysics were used to analyze a landslide, over 68% only employed the use of a single geophysical method in conjunction with geotechnical methods even though it is believed that there are benefits of using more than one. The study discussed in this paper uses a combination of ERT, HVSR, and MASW data to enhance the slope model inputs and therefore, a past study pertaining to each will be briefly explained.



In 2012, Junior et al. (2012) conducted a study on a slope in Ubatuba City, Brazil that contained unsaturated soils and had a history of landslide occurrences. MASW testing was selected as a key tool in the study. Results showed that when done concurrently with laboratory and in-situ testing, the Vs profile produced by MASW testing could be correlated with soil stiffness parameters and can be an effective tool in monitoring landslide prone areas. A case study was completed in 2016 over two fairly substantial landslide areas: Castagnola in La Spezia, Italy and Roccalbegna in Grosseto, Italy. This study found that HVSr can be used to understand the landslide geometry, i.e., the slip surface. (Pazzi et al., 2016) Another recent study was conducted in 2019 to evaluate the current state of the landslide in Brzozówka, Poland using ERT data in addition to geotechnical methods. ERT was selected as the only geophysical procedure due to its efficiency and overall popularity in slope stability analysis and drilling, while cone penetration testing, and laboratory testing were the chosen geotechnical procedures. Using numerical simulations, more specifically FEM, as the modeling software, the combination of ERT data and geotechnical testing allowed Pasiarb et al. (2019) to determine the saturation that would likely cause a slope failure.

This thesis presents a study on two unstable slopes in Arkansas where the use of geophysical data was attractive due to limited geotechnical data, complex soil profiles, and issues at each of the sites likely caused by the presence of water. Following this introduction, the methodology used at each of the sites is discussed including the available data and the types of slope models generated. The results will then be presented and discussed, followed by the conclusions drawn from this work.

## Methodology

### Site Backgrounds

Two unstable highway slopes located in Arkansas were the focus of this project. Both slopes show visible evidence of reoccurring slides in the form of soil heaving and pavement cracking. Site 1 is located on a portion of Highway 7 near Sand Gap Arkansas which is located in the Northwest Arkansas region. Sand Gap is situated in the Ozark Mountains which contains v-shaped valleys and steep hill slopes. The bedrock is made up of shale and sandstone layers that sharply dip down in some areas. This site shows signs of slope movement in the form of longitudinal cracking along the road pavement. Figure 2 shows the location of the site and the area where testing was conducted and Figure 3 shows evidence of longitudinal cracking.

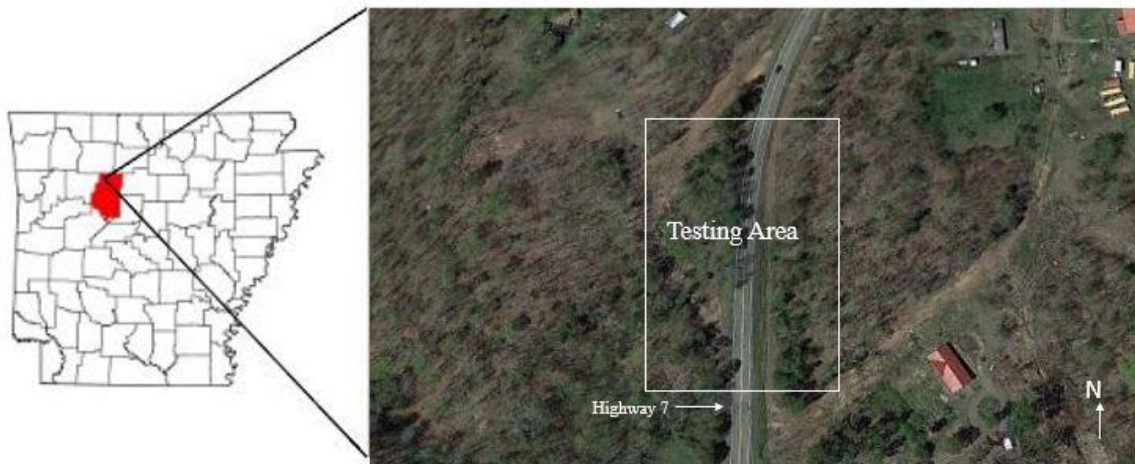


Figure 2- Sand Gap Testing Area (Used by permission from Salman Rahimi and retrieved from Google Earth)



Figure 3- Longitudinal Crack Located on Highway 7 (Used with Permission from Salman Rahimi)

The area of interest slopes from north to south and east to west. The steepest part of the area slopes to the southwest. The Arkansas Department of Transportation drilled four borings and installed a single inclinometer on the west side of the road. Borings could not be easily taken on the east side due to accessibility issues. These borings showed a layer of stiff clay underlain by sandstone and occasional shale. The boring logs reported that the top part of the bedrock was highly weathered. Since no borings were taken on the east side of the road, little is known about the stratigraphy upslope. There is also a spring located on the southwest corner of the site. ERT, MASW, and HVSR testing was completed on both the east and west sides of Highway 7. Figure 4 shows the locations of the borings and geophysical testing conducted at the site.

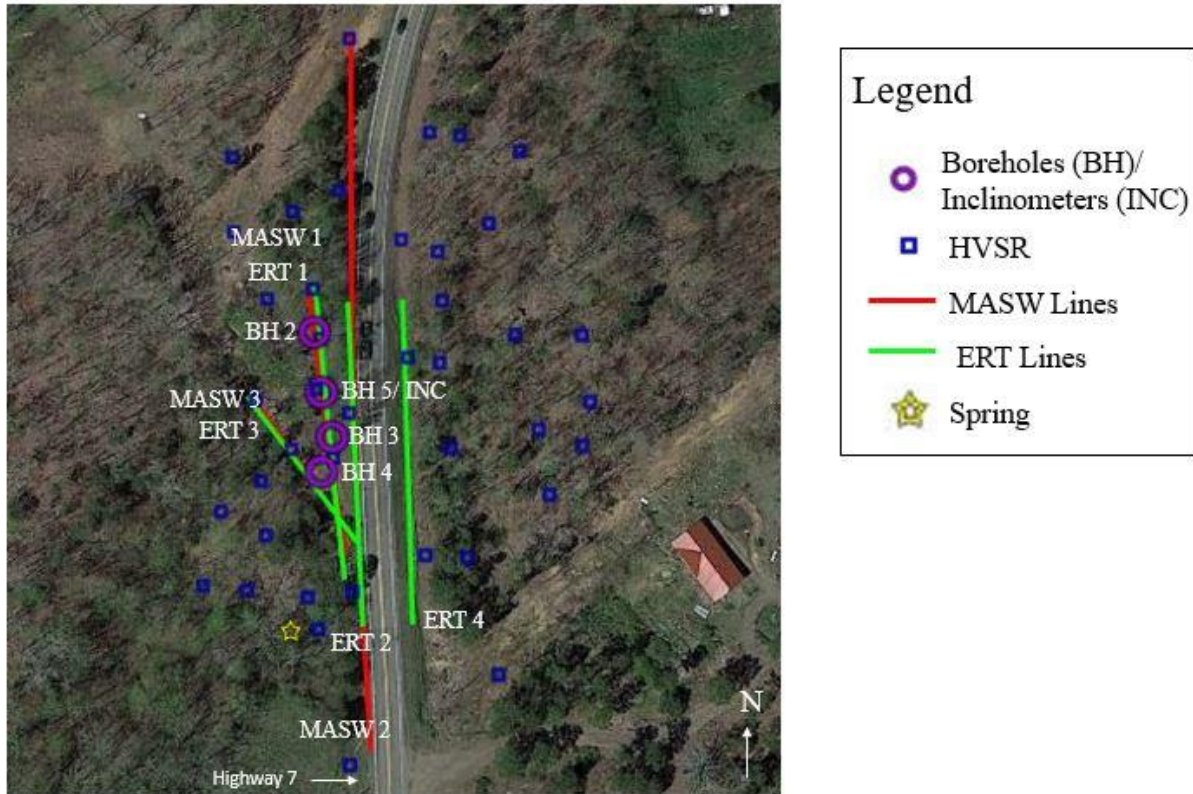


Figure 4- Testing Locations for Sand Gap (Retrieved from Google Earth)

A total of four ERT lines, three MASW lines, and 40 HVSR points were collected. Additionally, airborne light detection and ranging (LiDAR) data was used to obtain elevations for this site.

Site 2 is located north west of Ozark Arkansas on a part of the I-40 westbound lane. Ozark is located in the Northwestern region of Arkansas, situated roughly sixty miles southwest of the Sand Gap site. The area in question slopes south to north on a 30-40% grade. Evidence of a slide is visible in the form of longitudinal cracking in the I-40 westbound lane, deep soil cracking near the top of the slope, and soil heaving at the bottom of the slope. Figures 5 and 6 show the testing area and images of the soil and pavement cracking, respectively.



Figure 5- Testing Area for Ozark Site (Used with permission from Salman Rahimi and retrieved from Google Earth)

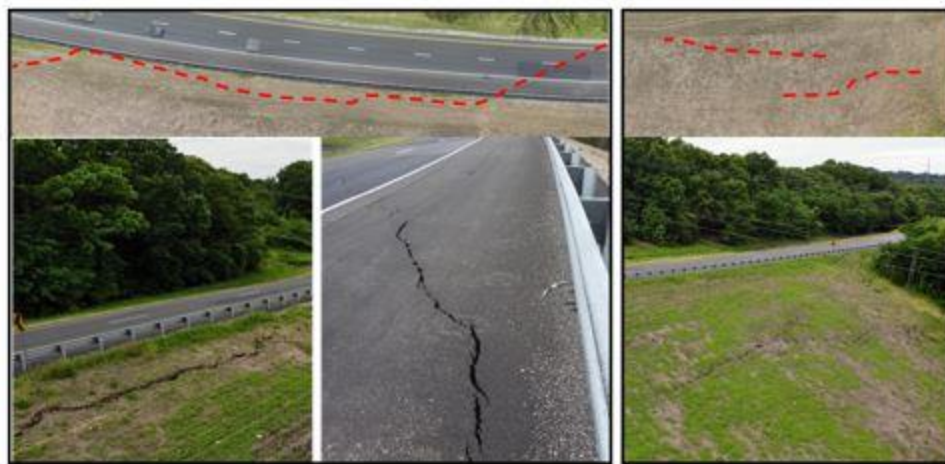


Figure 6- Longitudinal Pavement Cracking and Soil Cracking (Used with Permission from Salman Rahimi)

Eighteen borings were drilled throughout the site and showed that the soil profiles varies across the slope. The site consists mostly of clays of varying stiffness with pockets of sand, gravel, and boulders found throughout. The bedrock consists of shale underlain by sandstone. The top layering of shale is mostly weathered to highly weathered. There is a spring located on

the northeast corner of the site. It should be noted that in 2018 an attempt was made to restabilize the slope with the addition of encapsulated strand anchors.

In addition to the borings, five MASW lines, eight ERT lines, and seventy-seven HVSR points were also tested at the site. Figure 7 shows the locations of the borings and geophysical testing.



Figure 7- Testing Locations for Borings and Geophysics for Ozark (Retrieved from Google Earth)

A total of 6 inclinometers were installed on site, four before the anchors were installed and two after. Inclinometers 1-4 were installed prior to the anchor installation and Inclinometers 6 and 7 were installed after the anchors. Figure 7 shows the locations of each inclinometer. Additionally, handheld GPS was used to obtain elevations for this site.

## Analysis Methods

The 2D modeling software Slide by Rocscience was selected for the slope analysis due to its variety of methods, user friendly interface, and because it is a commonly used program.

Simplified Bishop, Simplified Janbu, and Morgenstern-Price were the limit equilibrium methods selected for analysis. Bishop Simplified method was investigated using both circular and non-circular failure methods; however, this thesis only includes the circular failure analysis. It should be noted that the non-circular method for Simplified Bishop showed lower FOSs than the circular method and presented slip surfaces similar to Simplified Janbu and Morgenstern-Price. Each site was broken up into various phases and will be discussed separately.

SPT correlations were used to obtain soil strength parameters. Equation 2 was used to find the undrained shear strength for each cohesive soil. (Race and Coffman, 2013)

$$s_u[\text{kPa}] = (N/8) * 47.88 \quad \text{Equation 2}$$

Table 3 shows the SPT to friction angle correlations used for this study and Table 4 shows the SPT correlations used to obtain unit weights for cohesive and non-cohesive soils. For simplification, clays with similar strength values were categorized according to Table 5. Additionally, bedrock was broken up into layers based on Rock Quality Density (RQD). Table 6 shows this classification.

Table 3: SPT to Friction Angle Correlations (Adapted from Meyerhof, 1956)

<b>Blow Count (N)</b>	<b>Soil Packing</b>	<b>Friction Angle (°)</b>
<4	Very Loose	<30
4-10	Loose	30-35
10-30	Compact	35-40
30-50	Dense	40-45
>50	Very Dense	>45

Table 4: SPT to Unit Weight Correlations (Adapted from Race and Coffman, 2013)

<b>Cohesive Soils</b>		<b>Cohesionless Soils</b>	
<b>Blow Count (N)</b>	<b>Unit Weight (kN/m<sup>3</sup>)</b>	<b>Corr. Blow Count (N<sub>60</sub>)</b>	<b>Unit Weight (kN/m<sup>3</sup>)</b>
<2	15.71	<4	11.00
2-8	18.85	4-10	14.14
8-16	20.42	10-30	17.28
>16	21.99	30-50	18.85
		>50	20.42

Table 5: Soil Description Classification based on Soil Strength

<b>Strength Values (kPa)</b>	<b>Soil Description</b>
0-25	Very Soft Clay
25-50	Soft Clay
50-100	Medium Clay
100-150	Stiff Clay
>150	Very Stiff Clay

Table 6: Bedrock Classification based on Rock Quality Density

<b>RQD (%)</b>	<b>Bedrock Description</b>
0-25	Weak
25-50	Medium
50-100	Competent

### **Sand Gap Site Analysis**

At the Sand Gap site two cross-sections were investigated in an attempt to find the true slip surface. One cross-section was taken perpendicular to the road through the main longitudinal crack in the pavement. This cut goes through BH 5 and will be referred to as “Perpendicular Line.” The second cross-section was taken down the steepest slope, northeast to southwest, and



intersects the crack in the road. This cut passes between BH 3 and BH 4 and will be referred to as “High Low Line.” Figure 8 shows the locations of the two cross-sections in relation to the geotechnical and geophysical data collected.

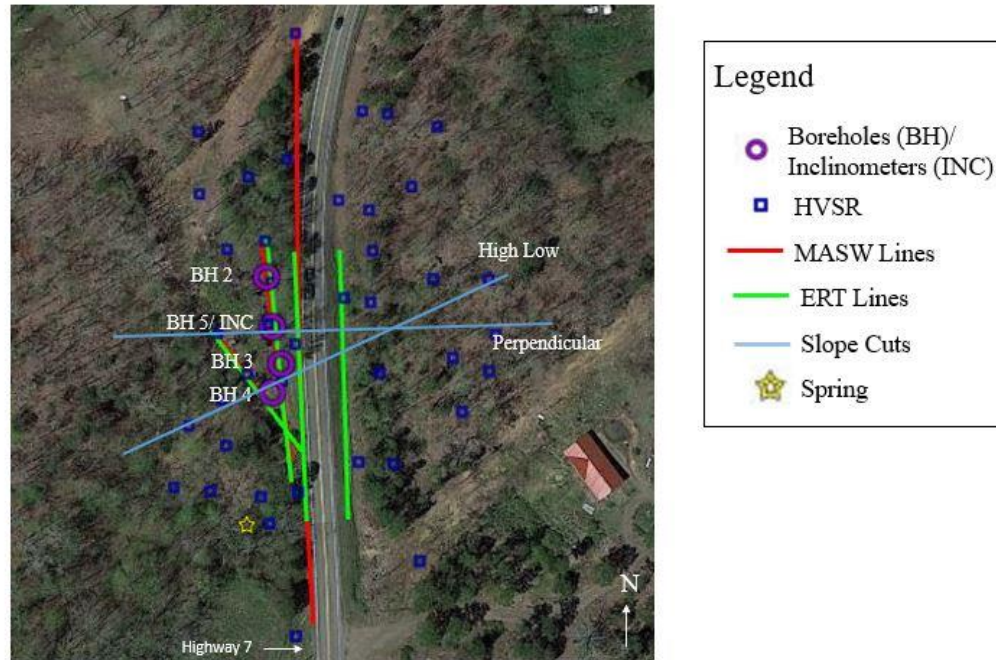







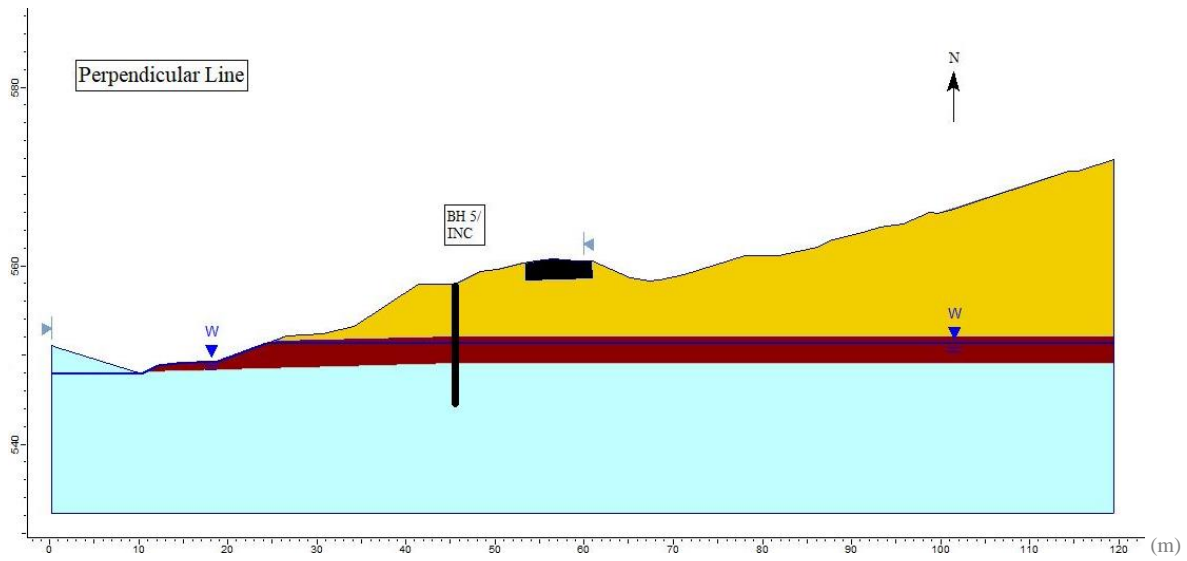
Figure 8- Cross-sections Taken for Slope Models (Retrieved from Google Earth)

This site analysis was divided up into two phases. Phase 1 consisted of a slope model that was created using only data from geotechnical boring logs. The Perpendicular Line model was created using BH 5 and the High Low model was created using BH 3 and BH 4. The soil layers for each model were based solely on the borings and were assumed to be horizontal. Additionally, the water table was extracted from a single boring and assumed to be horizontal as well. Phase 1 aimed to represent a traditional slope model using limited geotechnical data. As part of Phase 1, parametric studies were conducted for the medium sandstone and weak layers in each of the models since little information was known about the strength values. The slope

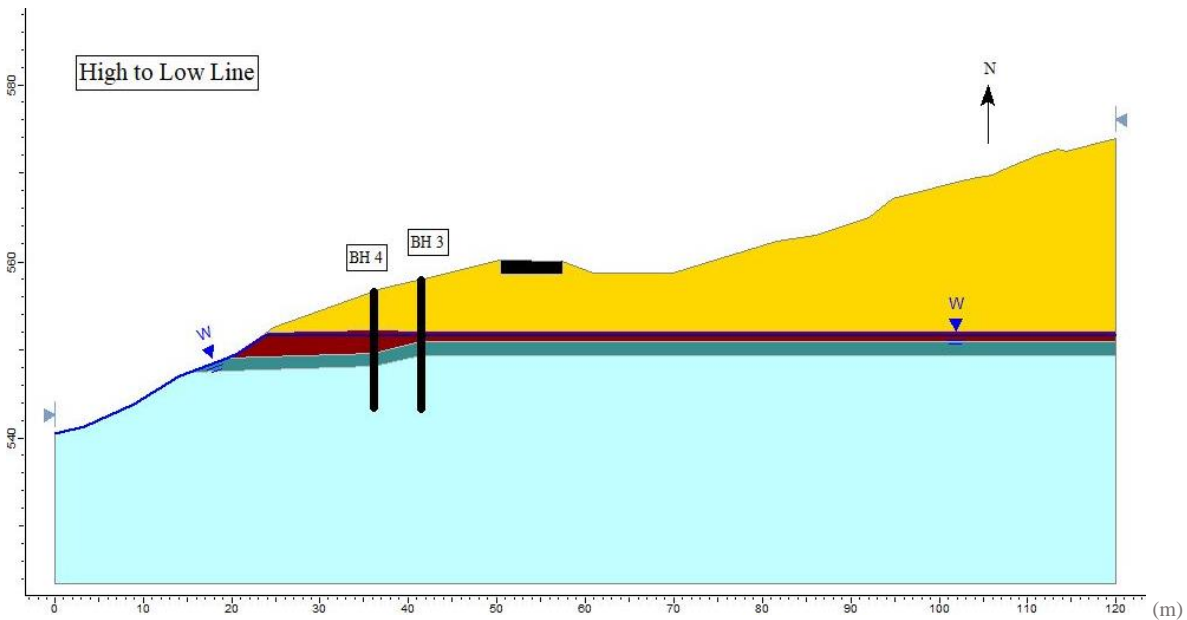
analyses for the Perpendicular Line were compared to the results from the inclinometer. It is noted that the slope analysis from the High Low Line was not compared to the inclinometer data since the slice did not cut through the inclinometer location. Table 7 provides the name and color coding of the soils found at the Sand Gap site and their properties and Figure 9 (a) and (b) show the Phase 1 cross sectional profiles for the Perpendicular Line and High Low Line, respectively. The black vertical lines in Figure 9 represent the locations of the borings used to derive the soil profile.

Table 7: Soil Strength Parameters for the Sand Gap Site

<b>Material Name</b>	<b>Color</b>	<b>Unit Weight (kN/m<sup>3</sup>)</b>	<b>Strength Types</b>	<b>Cohesion (kPa)</b>
Medium Clay		20.42	Undrained	59.85
Weathered (Medium) Sandstone		21.99	Undrained	Varies
Weathered (Weak) Layer		20.42	Undrained	Varies
Competent Sandstone		21.99	Undrained	1000
Asphalt		20.42	Undrained	75



(a)

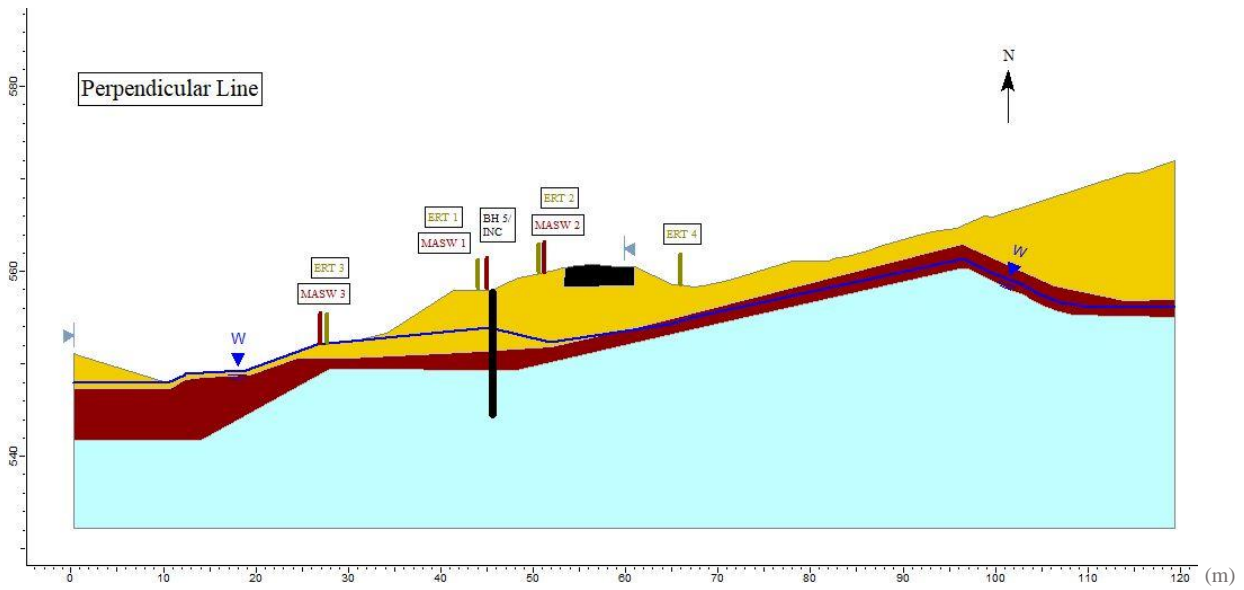


(b)

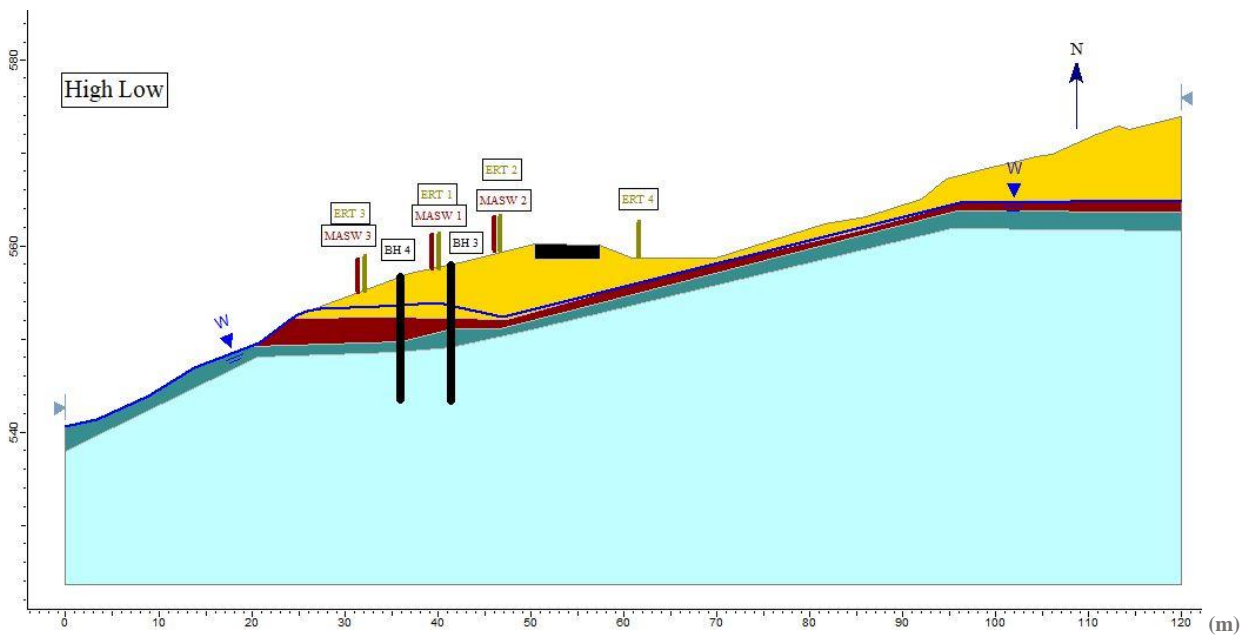
Figure 9- Models used for Phase 1 Slope Analysis for (a) Perpendicular Line and (b) High Low Line Cross-sections

The models created in Phase 2 included geophysical data in addition to the boring data. A total of four ERT lines, three MASW lines, and 39 HVSr points were tested across the site. The ERT data were primarily used to update water table information, while the MASW and HVSr

data were used to locate bedrock across the site. ERT was also used to confirm findings from the MASW and HVSR data in some cases. It should be noted that the data obtained from ERT Line 1 and MASW Line 1 were compared with the data from BH 2, BH 3, and BH 5 to test for accuracy and provide “ground truth”. Additionally, a distributed load of 108 kPa was placed on the road way to model how the traffic load affects the slope stability. This load was selected to simulate the worst case scenario of two loaded semi-trucks driving through at the same time. Parametric studies were also completed for both lines in Phase 2. Figure 10 (a) and (b) show the Phase 2 cross sectional profiles for the Perpendicular Line and High Low Line, respectively. Similar to previous figures, the black lines represent the locations of borings and the other labels represent locations where the geophysical testing was conducted. As evident in the figure, the addition of the geophysical information significantly changed the location of bedrock across the cross-sections and also updated the location of the water table.



(a)



(b)

Figure 10- Models used for Phase 2 Slope Analysis for (a) Perpendicular Line and (b) High Low Line Cross-sections

## Ozark Site Analysis

Two cross-sections were also taken at the Ozark site for slope stability modeling. The first cross-section, Line 1, is perpendicular to the road and intersects BH 12, BH 13, BH 14, and BH 15. The second cross-section, Line 2, is also perpendicular to the road, but is situated west of Line 1 and intersects BH 8, BH 9, BH 10, and BH 11. Figure 11 shows where the cross-sections are located on site in relation to the geotechnical and geophysical data collected.


















Figure 11- Slope Cross-sections for Ozark Site (Retrieved from Google Earth)

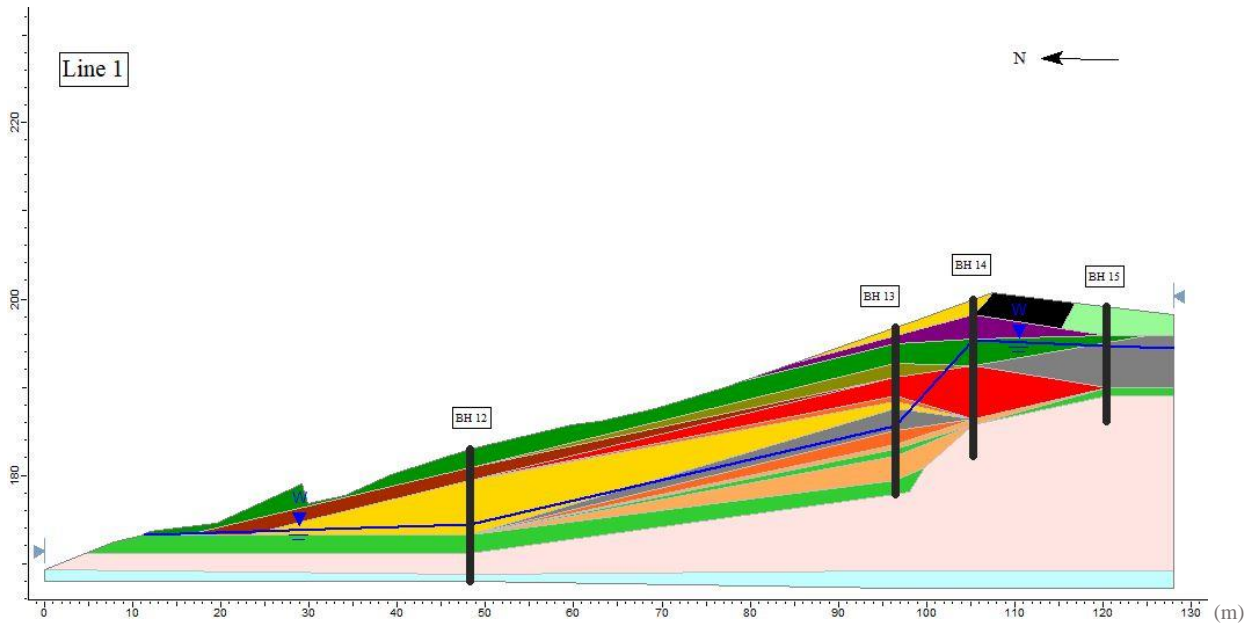
Similar to the Sand Gap site, the Ozark site was also broken up into phases. Phase 1 for Ozark contains only boring data and represents the slope before the anchors were installed. The results from Phase 1 were compared to the inclinometers that were installed before the anchors were installed to check for accuracy. Phase 1 also included a parametric study to examine the effects of soil strength for the weak layer consisting of highly weathered shale that was located on top of the competent shale. Table 8 shows the strength parameters for the soil present at the

Ozark site and Figure 12 (a) and (b) shows the Phase 1 cross sectional profiles for Line 1 and Line 2, respectively. Similar to previous profiles, the black vertical lines represent the locations of the borings.

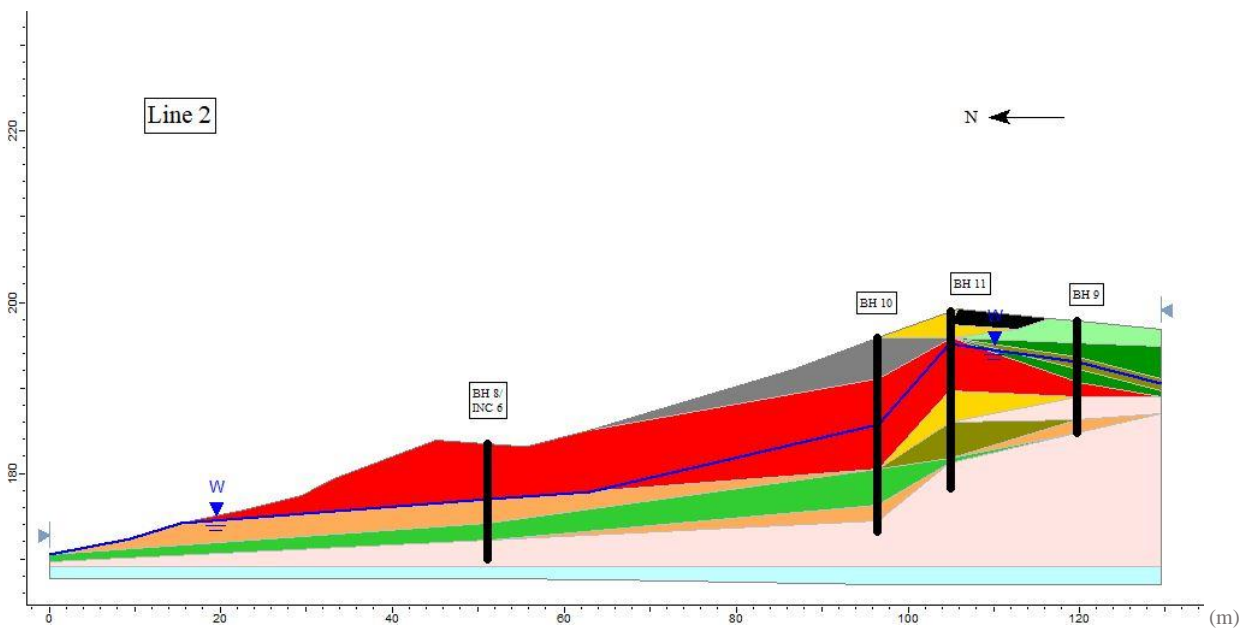
Table 8: Soil Strength Parameters for the Ozark Site

<b>Material Name</b>	<b>Color</b>	<b>Unit Weight (kN/m<sup>3</sup>)</b>	<b>Strength Types</b>	<b>Cohesion (kPa)</b>	<b>Phi (deg)</b>
Very Soft Clay		18.85	Undrained	23.95	N/A
Soft Clay 1		18.85	Undrained	38.91	N/A
Soft Clay 2		20.42	Undrained	47.88	N/A
Medium Clay		20.42	Undrained	59.85	N/A
Stiff Clay		21.99	Undrained	134.05	N/A
Very Stiff Clay		21.99	Undrained	215.46	N/A
Sand		14.14	Undrained	N/A	32
Dense Sand		18.85	Undrained	N/A	39
Gravel		17.28	Undrained	N/A	33
Weathered (Weak) Layer		20.42	Undrained	Varies	N/A
Weathered (Medium) Shale		20.42	Undrained	Varies	N/A
Competent Shale		21.99	Undrained	1000	N/A
Competent Sandstone		21.99	Undrained	1000	N/A
Fill Material		20.00	Undrained	75	N/A
Asphalt		20.42	Undrained	75	N/A





(a)

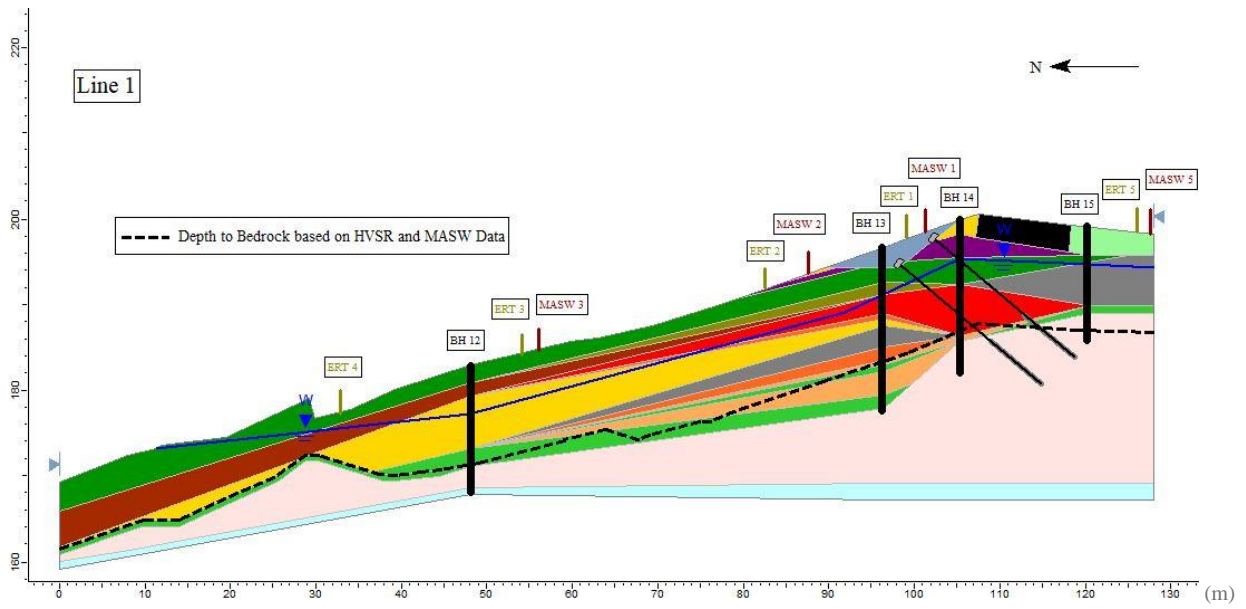


(b)

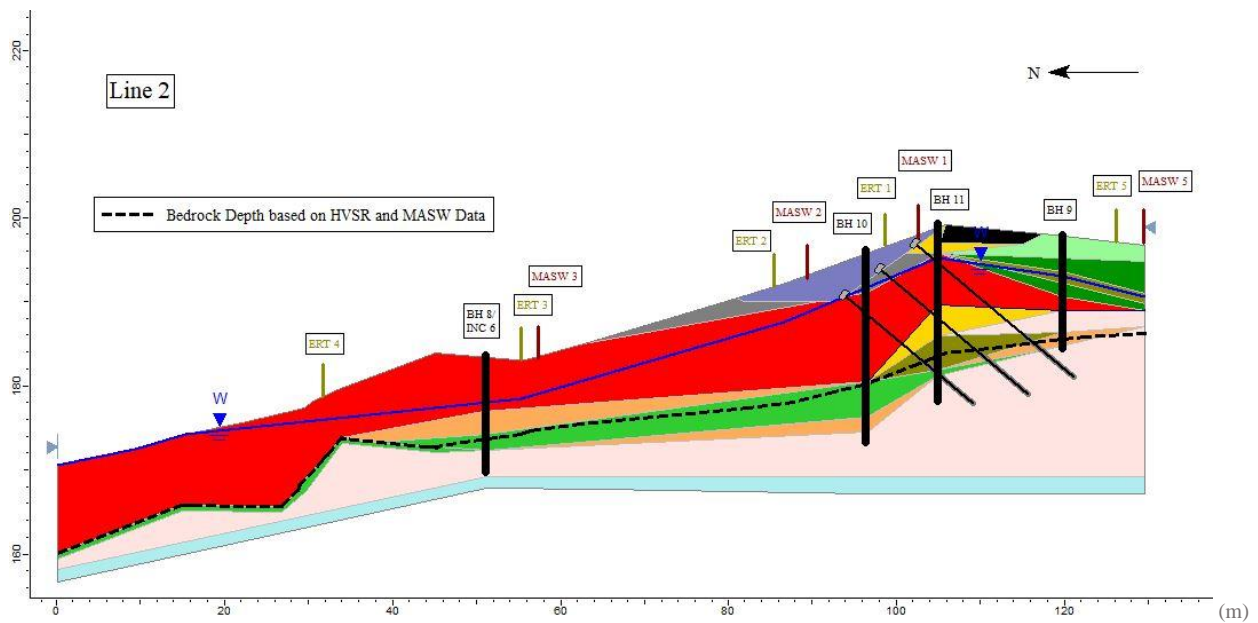
Figure 12- Models used for Phase 1 Slope Analysis for (a) Perpendicular and (b) High Low Line Cross-sections

Phase 2 modeled the site before the anchors were installed, but this time employed ERT, MASW, and HVSR data in addition to the data obtained from the borings. Phase 3 was used to

model the slope after the anchors were installed and used only borings to generate the soil profile. It should be noted that Line 1 cuts through an area with two anchors and Line 2 cuts through an area with three anchors. Finally, Phase 4 includes the addition of ERT, MASW and HVSR data after the anchors were installed. For further investigation, Phase 4 was broken up into two parts. Part 1 includes boring data and geophysical data after the anchors were installed without a traffic load and Part 2 includes boring data and geophysical data after the anchors were installed and the addition of a traffic load. Figure 13 (a) and (b) shows the cross sectional profiles for Line 1 and Line 2 used for Phase 4, respectively, when the anchors were in place.



(a)



(b)

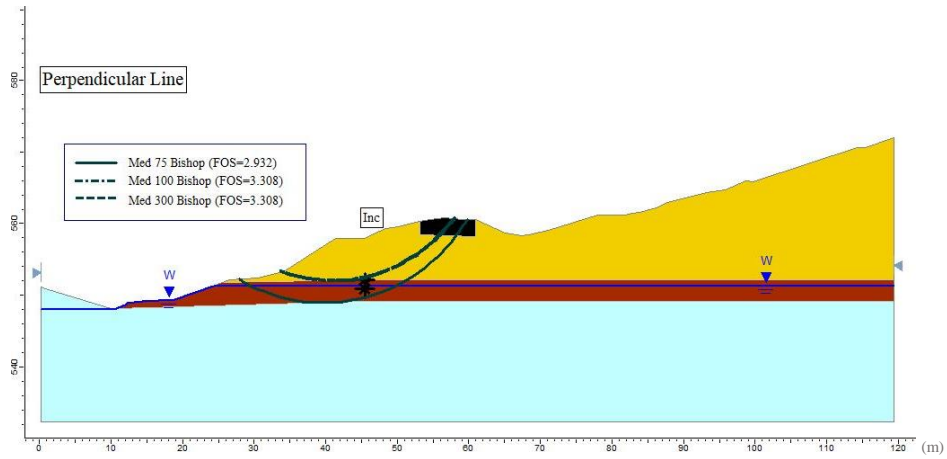
Figure 13- Models used for Phase 4 Slope Analysis for (a) Perpendicular and (b) High Low Line Cross Sections

## **Results and Discussion**

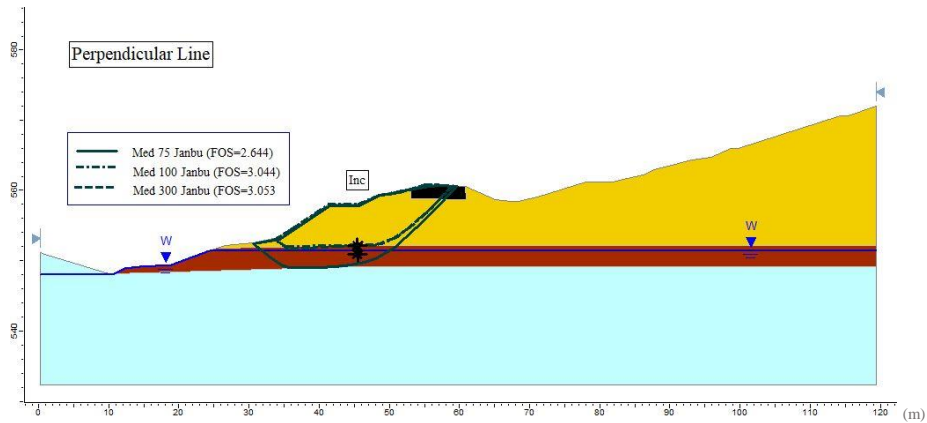
### **Sand Gap Site**

#### ***Perpendicular Line***

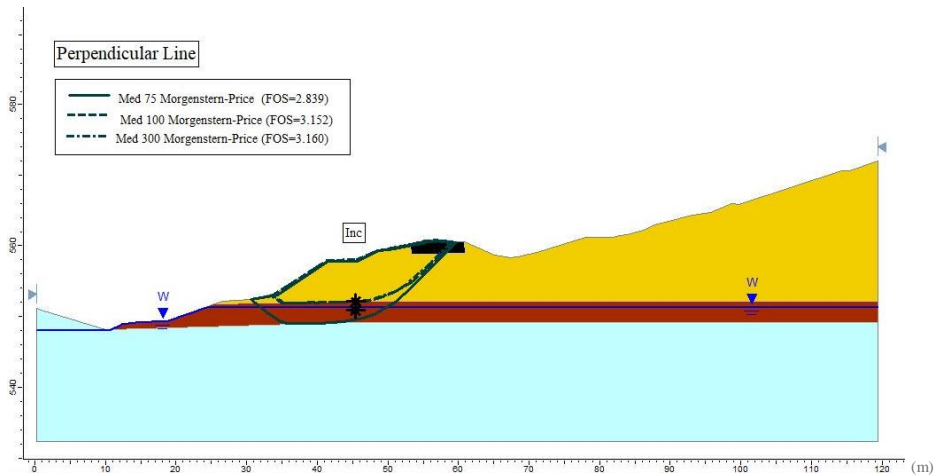
The two cross sections taken at the Sand Gap site will be discussed separately in this section, starting with the Perpendicular Line. Figure 14 shows the Phase 1, borings only, models for the perpendicular site using the Simplified Bishop method, Simplified Janbu method, and the Morgenstern-Price method. For this particular cross section, there were only 3 layers present: a medium clay (yellow), medium weathered sandstone (maroon), and competent sandstone (light blue). Based on the inclinometer data from the site, denoted in Figure 14 by asterisks, the slide seems to occur near the top of the medium sandstone layer; however, due to limited information from the boring logs, little is known about the strength properties of the medium sandstone layer. Therefore, for the Perpendicular Line cross section, a parametric study was conducted for Phase 1 for each of the methods. The selected undrained shear strength values for the medium weathered sandstone layer were 75 kPa, 100 kPa, and 300 kPa.



(a)



(b)



(c)

Figure 14- Parametric Study for Phase 1 Perpendicular Line using (a) Simplified Bishop, (b) Simplified Janbu, and (c) Morgenstern-Price Method

Figure 14 shows that when a value of 75 kPa is assumed for the medium sandstone layer, the failure surface slides along the medium and competent sandstone layer interfaces for all methods which is below where the inclinometer is reading the movement. Figure 14 also shows that when the medium sandstone layer is assumed to have a value of 100 kPa and 300 kPa, the failure surface shifts up to the medium sandstone and medium clay layer interface. These failure surfaces align closer to the movement zones reported from the inclinometer. Regardless of the value or method selected for the Phase 1 Perpendicular Line, all of the FOSs are far higher than 1.0 and therefore, according to these analyses, the slope is not failing. One explanation of this discrepancy with what is physically observed could be that there is a weaker zone along the top of the medium sandstone layer (not captured in the boring log) leading to a reduction in FOS. Before exploring this possibility, a more accurate representation of the slope was generated using the geophysical data. It was presumed that this more detailed analysis would likely provide a different FOS and could result in more reasonable estimates of the slope behavior.

The Phase 2 models were created using data collected from the various ERT and MASW lines and HVSR points collected over the site. Data collected from ERT Line 1 and MASW Line 1 were compared to BH 2, BH 3, and BH 5. Figure 15 shows the borings overlaid on the ERT Line 1 plot. The dotted line shows the estimated bedrock depth based on MASW and HVSR data.

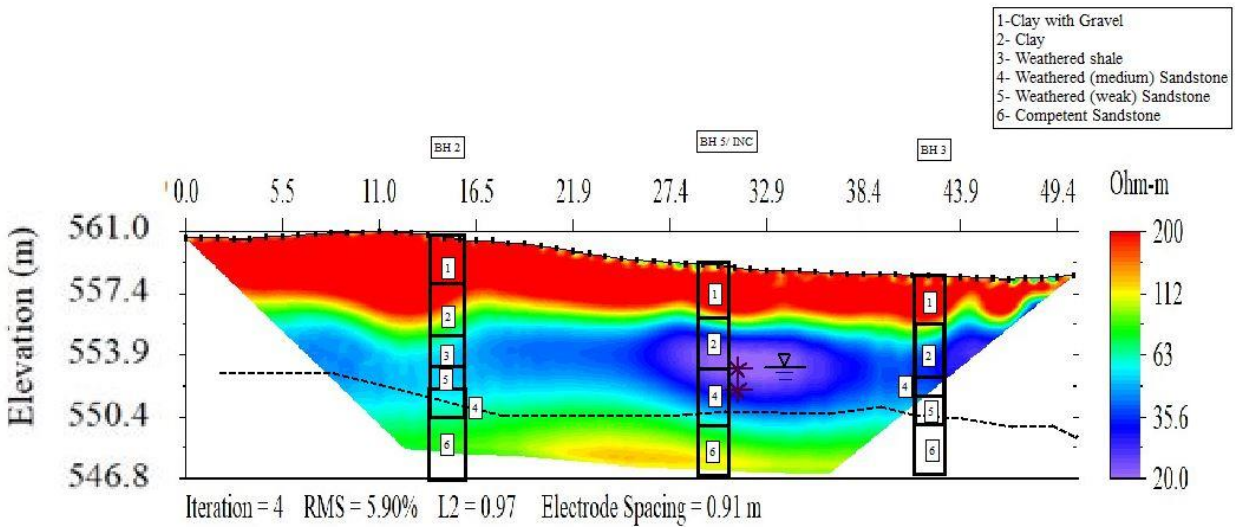


Figure 15-ERT Line 1 and MASW Line 1 Bedrock Line with Borings overlaid (Used with Permission from Weston Koehn)

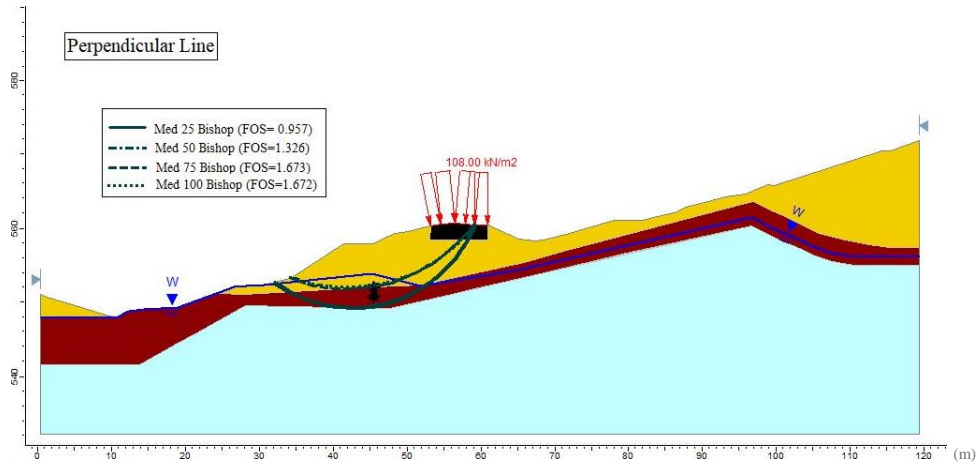
The borings were overlaid on the ERT plot so that connections could be made between the colors, resistivity values, in the plot and the soil layers present on site. Figure 15 allows us to interpret the following:

- The top red layer of the plot is likely a dry portion of the medium clay layer
- The purple area near BH 5 is likely the water table; however, there is potential that the top of the light blue line represents soil saturated above the water table due to capillary rise.
- The green and yellow coloring at the bottom of the plot suggest the absence of water and indicate the potential of bedrock. This also agrees with the bedrock line (dotted line) given by MASW and HVSR data.

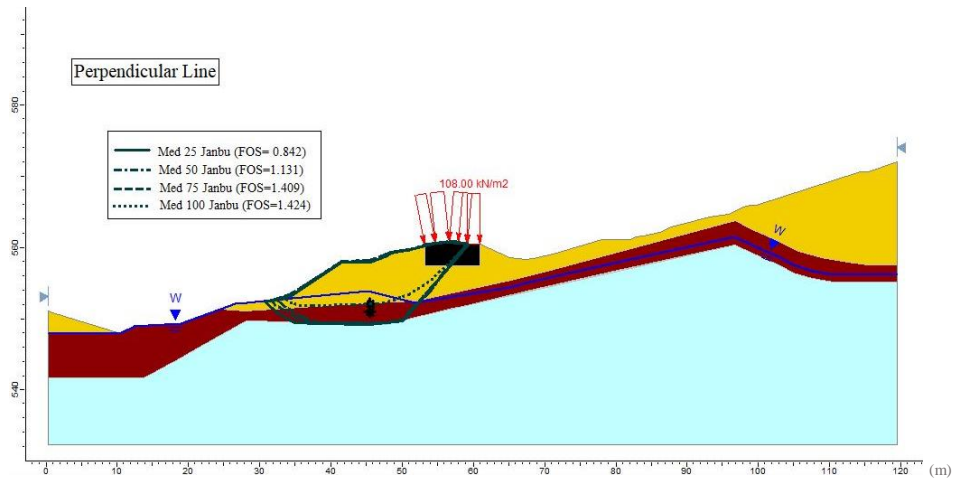
The conclusions drawn from Figure 15 were used to interpret the other ERT lines on site. The geophysical data combined with the boring data were used to create the Phase 2 models shown in

Figure 16. It should be noted that an additional traffic load of 108 kPa was added to the road to simulate the worst case scenario of two loaded semi-trucks driving through at the same time. Additionally, 25 kPa and 50 kPa values were added to the medium sandstone parametric study to lower the value and induce a failure. To simplify the figures, the 300 kPa value slip surface was omitted because it had the same slip surface as the 100 kPa value.

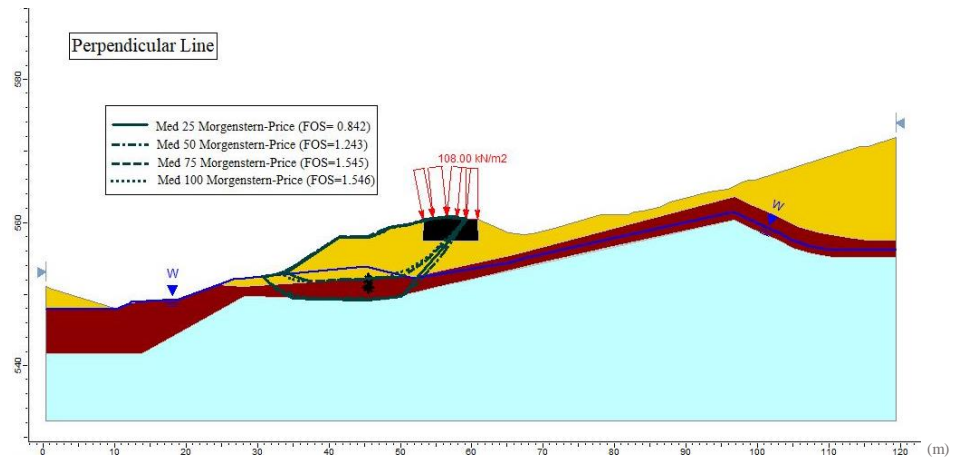




(a)



(b)

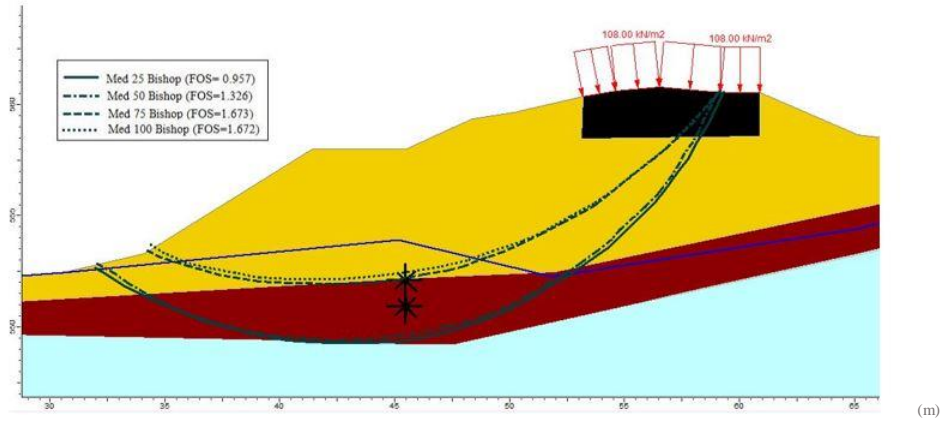


(c)

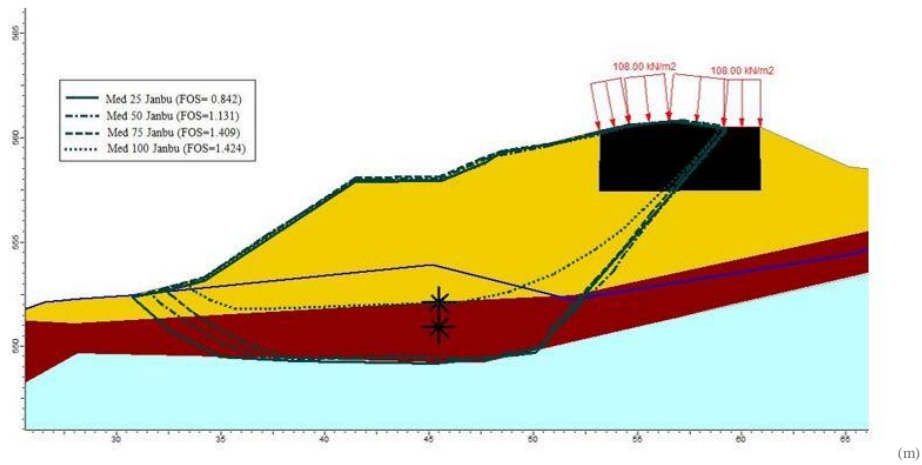
Figure 16- Parametric Study for Phase 2 Perpendicular Line using (a) Simplified Bishop, (b) Simplified Janbu, and (c) Morgenstern-Price Method

The biggest differences between the Phase 1 and Phase 2 model layouts occur on the east side, uphill, of the road. The additional geophysical data provided clarity to the location of bedrock on the east side of the road. While Phase 1 could only assume that the bedrock was horizontal across the slope, the MASW and HVSR data suggests that the bedrock is sloped. The failure surfaces show some minor changes from Phase 1 to Phase 2. Including the updated bedrock information however, reduced the FOSs by 43-53%

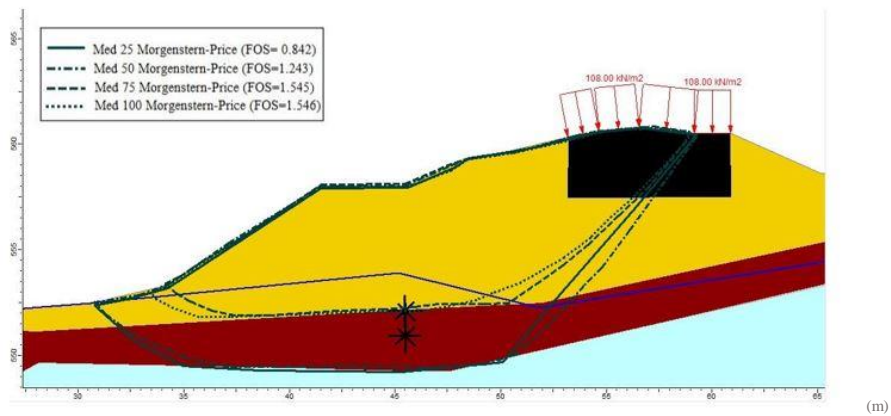
A zoomed in version of each of the Phase 2 models was created to be able to better compare each slip surface to the inclinometer reading. These are displayed in Figure 17. The black asterisks represent the lower and upper bounds of the movement based on the inclinometer readings.



(a)



(b)

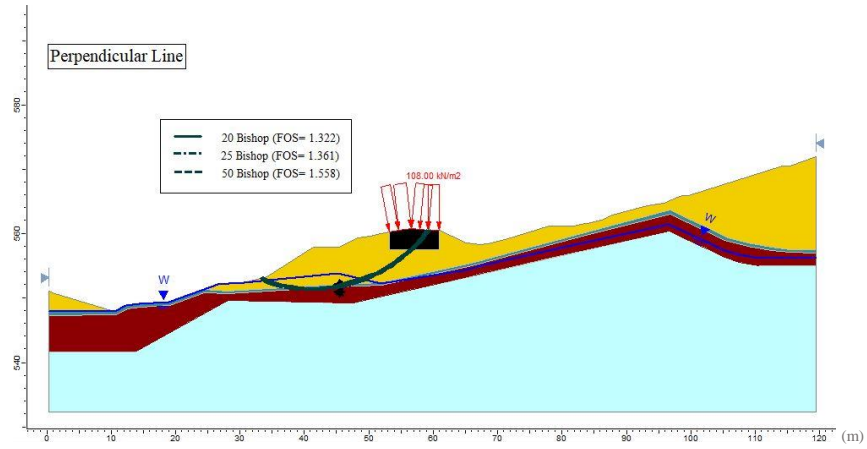


(c)

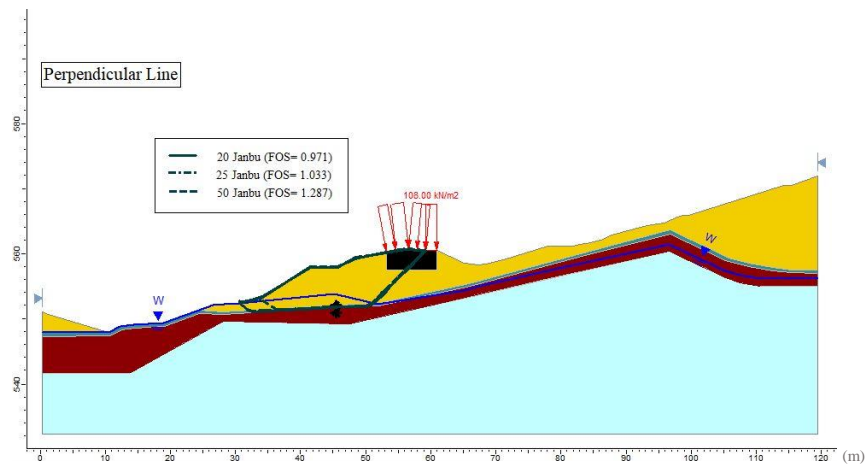
Figure 17- Parametric Study Zoomed in for Phase 2 Perpendicular Line using (a) Simplified Bishop, (b) Simplified Janbu, and (c) Morgenstern-Price Method

After the addition of geophysical data and the traffic load, the slip surface for the 75 kPa strength value shifted up from the medium and competent sandstone interface to the medium sandstone and medium clay interface for Simplified Bishop and Morgenstern-Price methods. For Janbu it remained the same. Another key note is that when the strength values of the medium sandstone layer were reduced until failure occurred, the slip still occurred along the medium and competent sandstone interface, which is still several meters below where the inclinometer detected the slip surface. This is due to the fact that the entire layer was reduced in strength as opposed to the top few feet of the layer which is likely closer to the actual scenario where weathering occurs.

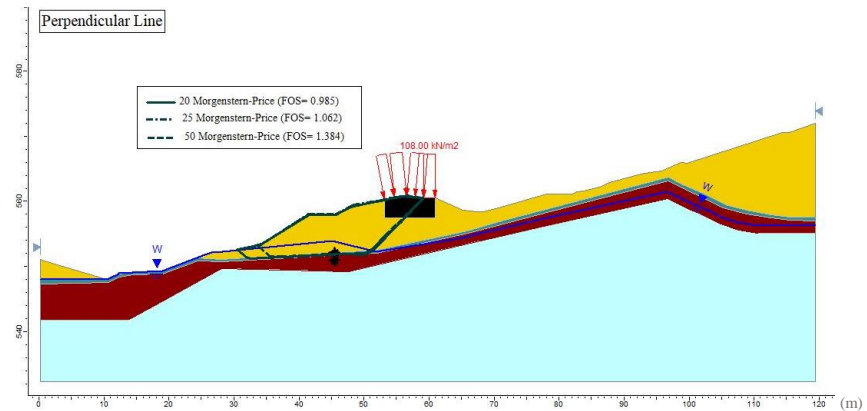
In an effort to examine the scenario where only the top portion of the layer was weakened from weathering, an additional model was added to Phase 2 for the Perpendicular Line. A 0.6 meter highly weathered weak layer was added to the model at the top of the medium sandstone layer. A new parametric study was conducted to examine different undrained strength values for the new weak layer. The strength values tested were 20 kPa, 25 kPa, and 50 kPa. For this study, the medium sandstone layer was given a strength of 75 kPa. Figure 18 shows the results from the Phase 2 with Weak Layer for the Perpendicular Line for each method and Figure 19 shows a zoomed in version of the slip surfaces in Figure 18 to better compare the failures to the inclinometer data. The inclinometer data is represented by black asterisks.



(a)

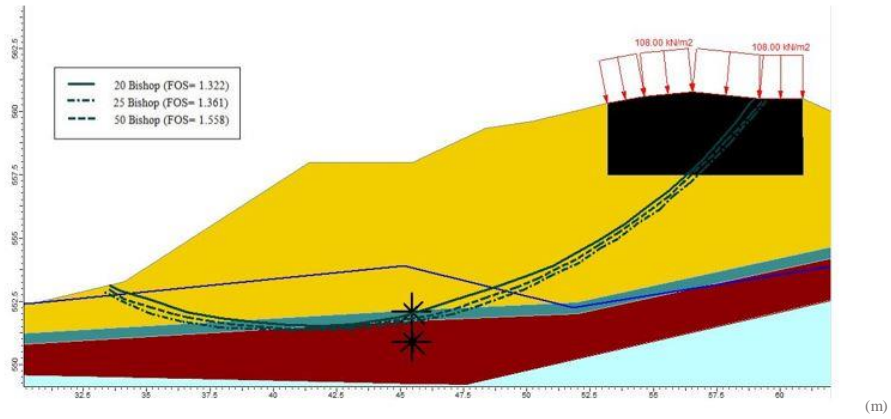


(b)

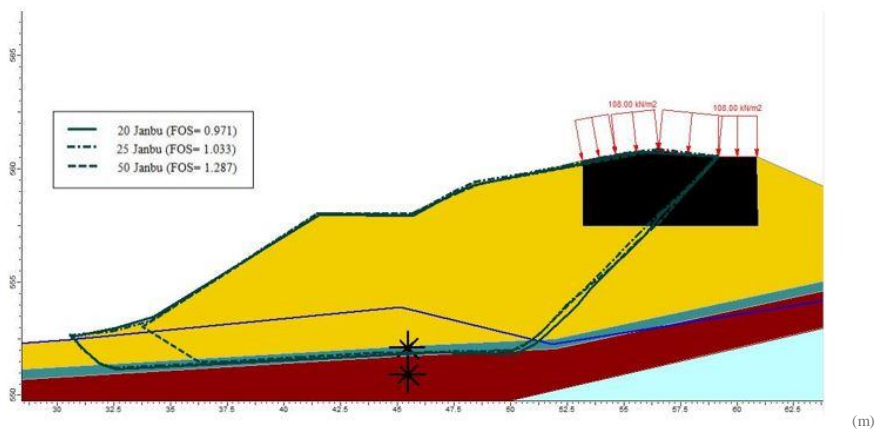


(c)

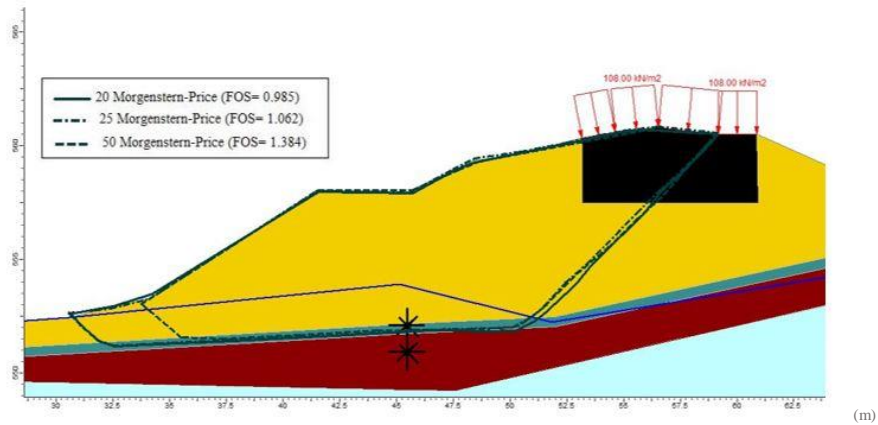
Figure 18- Parametric Study for Phase with Weak Layer Perpendicular Line using (a) Simplified Bishop, (b) Simplified Janbu, (c) Morgenstern-Price Method



(a)



(b)



(c)

Figure 19- Parametric Study Zoomed in for Phase 2 after addition of Weak Layer Perpendicular Line using (a) Simplified Bishop, (b) Simplified Janbu, (c) Morgenstern-Price Method

The addition of the weak layer shifted the failure to fall within the slip area indicated by the inclinometer. However, it is likely that the weak layer is deeper than 0.6 m given the movement zone in the inclinometer. Simplified Bishop method has FOSs all greater than 1.3, the accepted design FOS for this type of slope, which suggests that the slope would be safe assuming a circular failure surface. Janbu Simplified and Morgenstern-Price methods have nearly identical slip surfaces to one another and have FOSs close to or less than 1.0 for strength values of 20 kPa and 25 kPa. This suggests that the top layer of the medium sandstone, could contain a highly weathered (weak) seam that is contributing to the slope failure. While the RQD% was 44 for the location of movement indicated by the inclinometer, the slope model indicates that the equivalent strength for this rock quality is likely lower than what might be expected. The FOSs from Phase 1, Phase 2, and Phase 2 with Weak Layer have been combined into Table 9 to provide a comparison of the analyses results.

Table 9: FOS Tabulations for Sand Gap Site Perpendicular Line

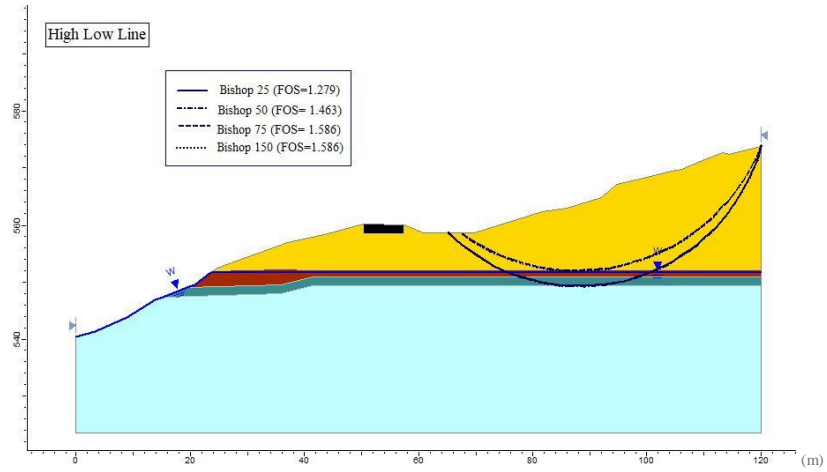
<b>Perpendicular Line Phase 1</b>	<b>Medium Sandstone Layer Strength (kPa)</b>	<b>Simplified Bishop</b>	<b>Simplified Janbu</b>	<b>Morgenstern-Price</b>
	<b>75</b>	2.932	2.644	2.839
	<b>100</b>	3.308	3.044	3.152
	<b>300</b>	3.308	3.053	3.16
<b>Perpendicular Line Phase 2</b>	<b>Medium Sandstone Layer Strength (kPa)</b>	<b>Simplified Bishop</b>	<b>Simplified Janbu</b>	<b>Morgenstern-Price</b>
	<b>25</b>	0.957	0.842	0.842
	<b>50</b>	1.326	1.131	1.243
	<b>75</b>	1.673	1.409	1.545
	<b>100</b>	1.672	1.424	1.546
	<b>300</b>	1.672	1.425	1.548
<b>Perpendicular Line Phase 2 with added Weak Layer</b>	<b>Added Weak Layer Strength (kPa)</b>	<b>Simplified Bishop</b>	<b>Simplified Janbu</b>	<b>Morgenstern-Price</b>
	<b>20</b>	1.322	0.971	0.985
	<b>25</b>	1.361	1.033	1.062
	<b>50</b>	1.558	1.287	1.384

### *High Low Line*

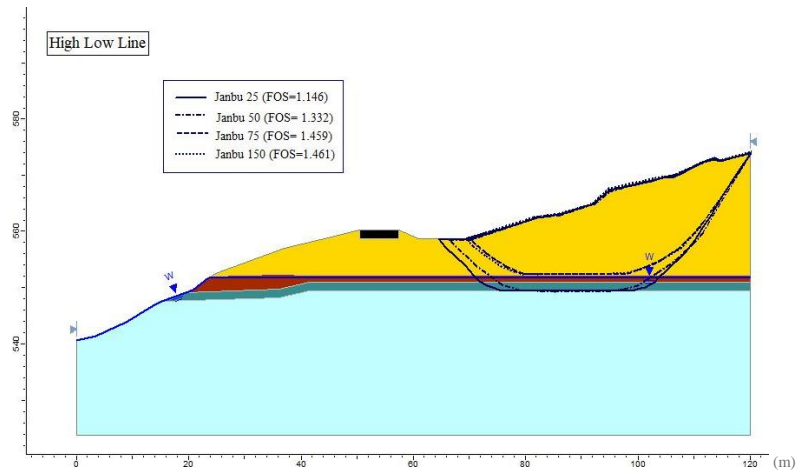
The High Low Line contains the same layers as the Perpendicular Line with the addition of a weak layer (dark blue) that appears between the medium and competent sandstone layers. There was not an inclinometer for the High Low cross-section, and therefore, the results were used to examine the influence of the addition of geophysical data and traffic load on the FOSs and slip surface locations. Figure 20 presents the parametric study conducted for the weak layer for the Phase 1 High Low Line using all three analysis methods. The undrained shear strength values used for the study were 25 kPa, 50 kPa, 75 kPa, and 150 kPa. A wide range was selected since little to no information was known about the layers true strength values. It should be noted that the medium sandstone layer strength also varied with the weak layer strength values to



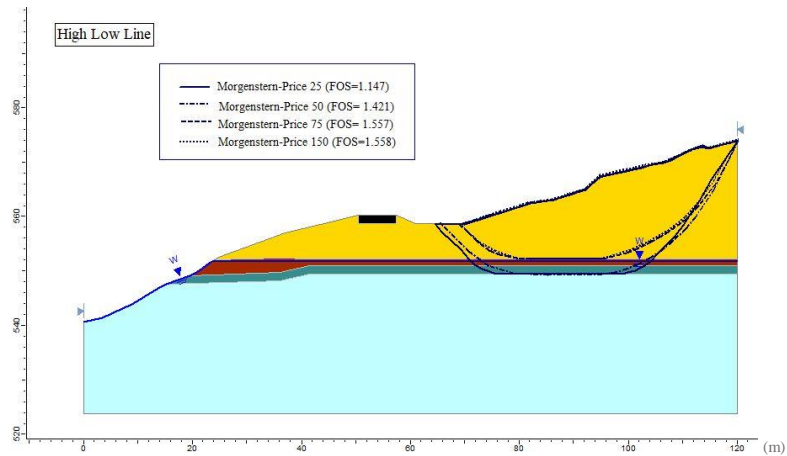
ensure that it was always stronger than the weak layer. For weak layer values of 25 kPa and 50 kPa the medium sandstone layer was assumed to have a value of 75 kPa. For a weak layer value of 75 kPa the medium sandstone layer was given a value of 100 kPa, and for the weak layer having a strength value of 150 kPa the medium sandstone layer was given a value of 300 kPa.



(a)



(b)

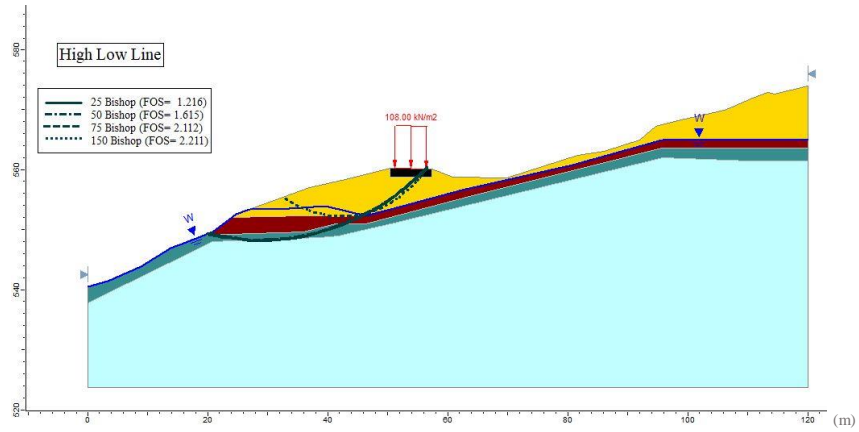


(c)

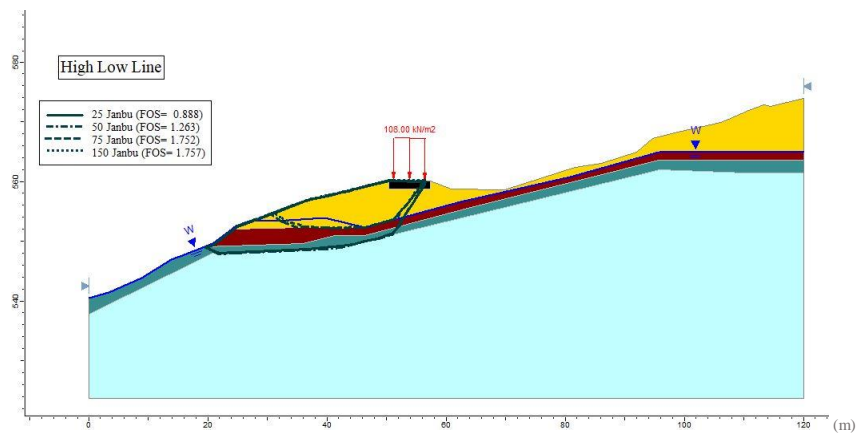
Figure 20- (a) Parametric Study for Phase 1 High Low Line using (a) Simplified Bishop, (b) Simplified Janbu, and (c) Morgenstern-Price Method

Figure 20 shows that the failures for all studies occur east of the road. Each method shows that when the weak layer is given a strength value of 50 kPa or lower, the failure surface occurs along the weak and competent sandstone layer interface; however, when the weak layer value is assumed to be 75 kPa or higher, the failure surface shifts up to the medium sandstone and medium clay layer interface. It should be noted that this shift could be occurring due to the increase in the medium sandstone layer strength that could be too strong for a failure to occur through it in this location. While several of the FOS values were below 1.3, the type and location of the failure surface in the model does not match the observed field conditions.

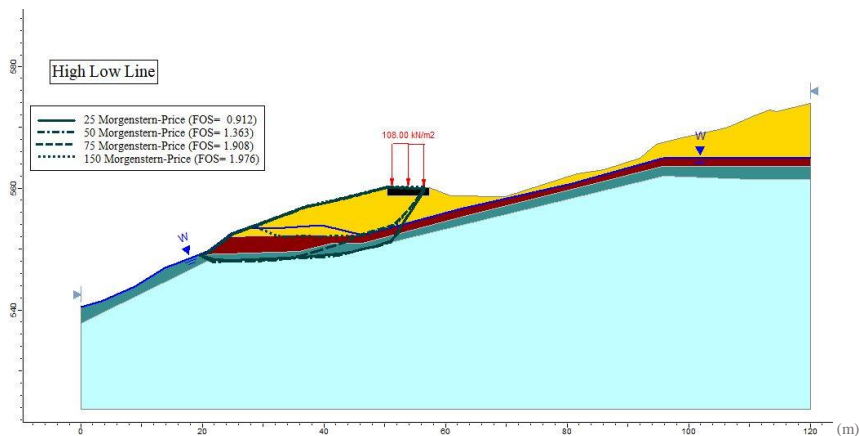
Similar to the Perpendicular Line, Phase 2 was created by adding geophysical data and traffic loading to the High Low boring data in an attempt to better represent true site conditions. Figure 21 shows the Phase 2 models for the High Low Line for each of the analysis methods.



(a)



(b)



(c)

Figure 21- Parametric Study for Phase 2 High Low Line using (a) Simplified Bishop, (b) Simplified Janbu, (c) Morgenstern-Price Method

A drastic shift in the slide location for all scenarios occurred after the addition of the geophysical data and traffic loading. In Phase 1 the slides were occurring east of the road and in Phase 2 the slides were occurring beneath and just west of the road, which better matched the observed movement and pavement cracking in the field. The location shift also affected the interface on which some of the slides occurred. For example, in the Morgenstern-Price model in Phase 1, the 75 kPa failure surface occurred at the medium sandstone and medium clay interface, but in the Phase 2 model, the failure occurred along the weak and competent sandstone interface. Additionally, the FOSs lowered from Phase 1 to Phase 2 and dropped below 1.0 for the 25 kPa scenario for Simplified Janbu and Morgenstern-Price.

The transformation of the Phase 1 to Phase 2 models suggest that the addition of geophysics on a site where boring information is limited could drastically affect the slope analysis results. Table 10 shows the fact FOSs for all the scenarios for the Phase 1 and Phase 2 High Low Line.

Table 10: FOS Tabulations for Sand Gap Site High Low Line

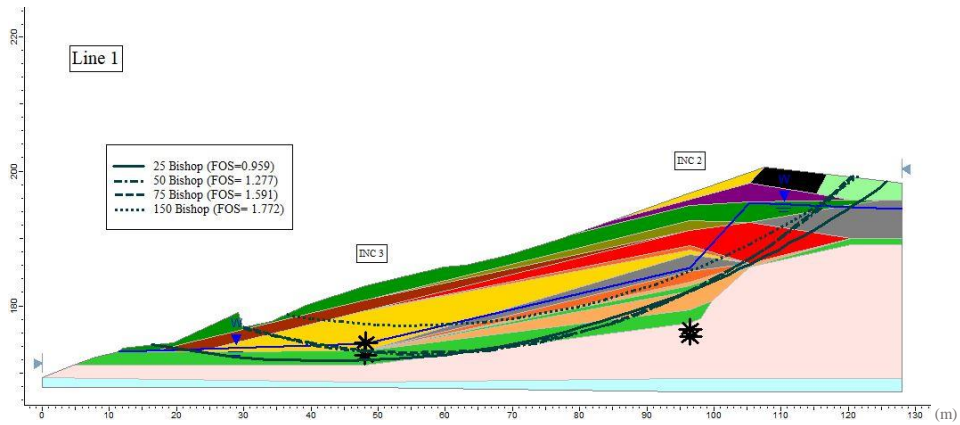
<b>High Low Phase 1</b>	<b>Weak Layer Strength (kPa)</b>	<b>Simplified Bishop</b>	<b>Simplified Janbu</b>	<b>Morgenstern- Price</b>
	<b>25</b>	1.279	1.146	1.147
	<b>50</b>	1.463	1.332	1.421
	<b>75</b>	1.586	1.459	1.557
	<b>150</b>	1.568	1.461	1.558
<b>High Low Phase 2</b>	<b>Weak Layer Strength (kPa)</b>	<b>Simplified Bishop</b>	<b>Simplified Janbu</b>	<b>Morgenstern- Price</b>
	<b>25</b>	1.216	0.888	0.912
	<b>50</b>	1.615	1.263	1.363
	<b>75</b>	2.112	1.752	1.908
	<b>150</b>	2.211	1.757	1.976

## **Ozark Site**

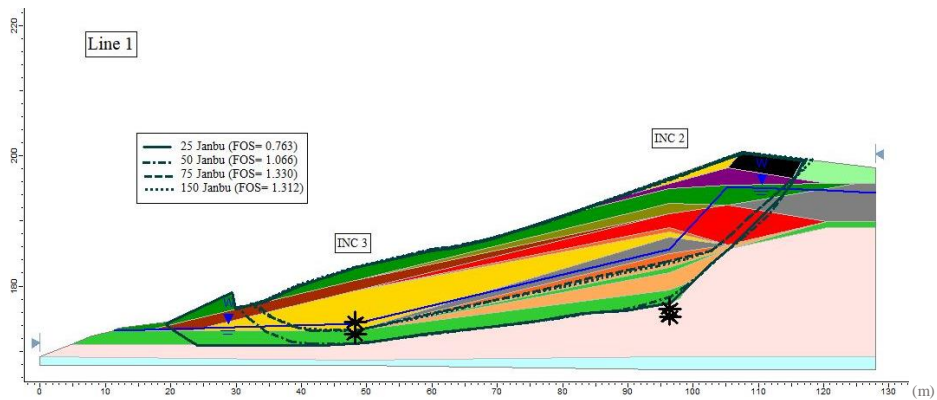
### ***Line 1***

Figure 22 shows the Phase 1, borings only, model for Line 1. Line 1 contains many different soil layers across the slope, but the important layers have been identified as the highly weathered shale layer (light green), medium shale layer (light orange), and competent shale layer (light pink), with the weak layer being the most critical. Little information is known about the strength properties of the shale layers and therefore, a parametric study was completed to analyze the slope behavior over a range of potential strength values. It should be noted that as the weak layer values changed in the parametric study so did the medium shale. The following are the weak and medium shale strength combinations used in the parametric study, respectively: 25 kPa and 75 kPa, 50 kPa and 75 kPa, 75 kPa and 100 kPa, and 150 kPa and 300 kPa.

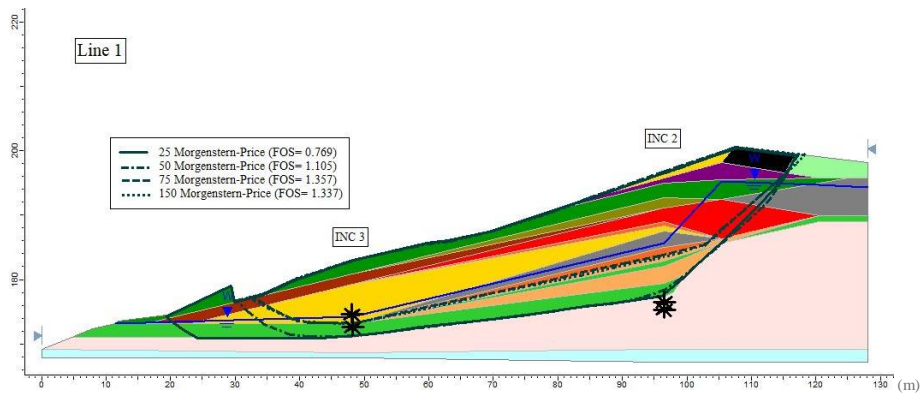
It should also be noted that Line 1 did not go directly through any inclinometers and therefore, data from nearby inclinometers were used and are shown in the figures by black asterisks. Although it appears that the movement zone in Inclinometer 2 is within the competent shale on Line 1, the zone fell within a weak layer in the boring where the inclinometer was located. Additionally, the boring, BH 13, used to generate the Line 1 soil profile in the location where the inclinometer is noted was terminated at the deepest point of the weak layer. The bedrock location for the competent shale was assumed in that location based on adjacent borings and because there was no information below that point. Therefore, it is possible that the inclinometer could actually be in weak layer on the Line 1 profile shown here.



(a)



(b)



(c)

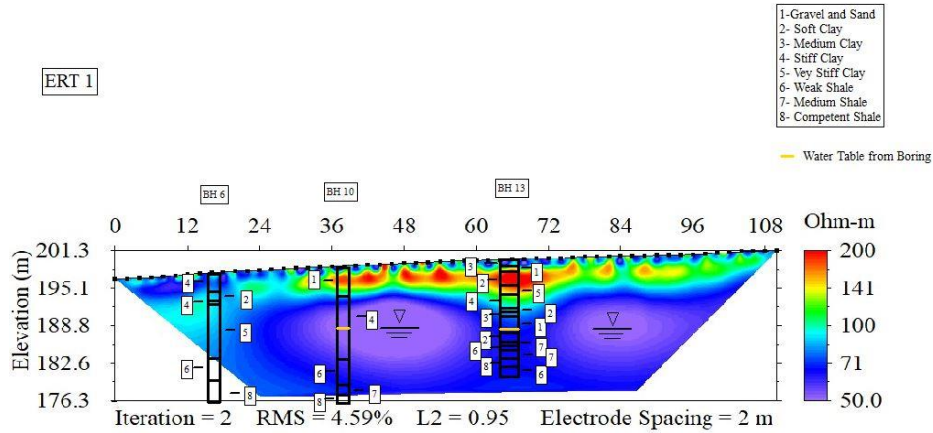
Figure 22- Parametric Study for Phase 1 Line 1 using (a) Simplified Bishop, (b) Simplified Janbu, (c) Morgenstern-Price Method

Figure 22 shows that when the weak layer is given a strength value of 50 kPa or less that the failure surface occurs along the weak and competent shale interface. Additionally, the FOSs are low, some even below 1.0, which suggest that a failure is likely to happen if the strengths are truly this low. If the strength value is 75 kPa or higher, the failure location tends to shift up to the weak layer and clay interface and the FOSs are greater than 1.3 which is the acceptable design value.

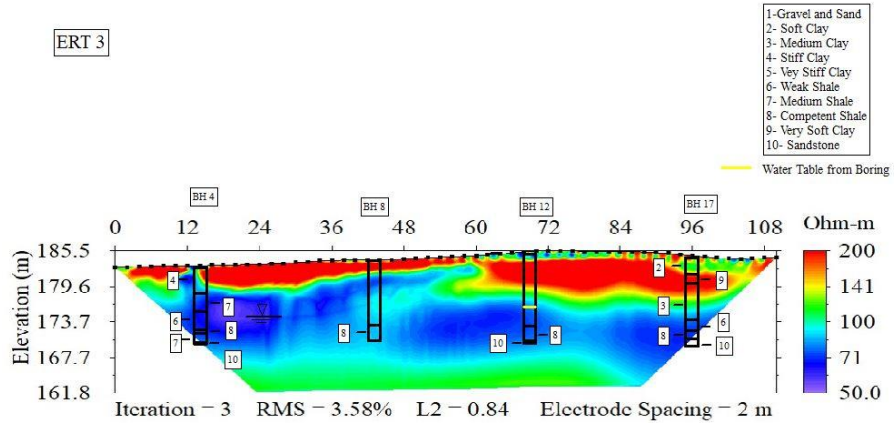
As mentioned previously, the inclinometers are located several meters away from Line 1 and therefore, the movement zones are shown by the inclinometers may not be exactly where the sliding was truly occurring. Also, Inclinometer 2 suggests that the failure is occurring in the competent shale. This is a result of two limitations to our model. 1) Line 1 does not cut directly through the inclinometer location. It is located roughly 50 meters east of Inclinometer 2, and therefore, the elevation at which the slide is occurring could change across that distance. 2) At the specific location where the inclinometer intersects Line 1, the depth to competent bedrock is unknown from the borings. The drilling ended in a weak layer and it is believe that the slide is occurring along the weak and competent shale interface. For these two reasons, the data from Inclinometer 2 was only used as a general comparison for Line 1.

The Phase 2 models were created using data from the various ERT and MASW lines and HVSR points collected over the site. Data collected from ERT Line 1 was compared to BH 6, BH 10, and BH 13, data collected from ERT Line 3 was compared to BH 4, BH 8, BH 12, and BH 17, and data collected from ERT Line 8 was compared to BH 12 to see what further conclusions could be deduced about the soil layering and water table between borings. Figure 23 shows the ERT plots for ERT 1, ERT 3, and ERT 8 with overlaid borings.

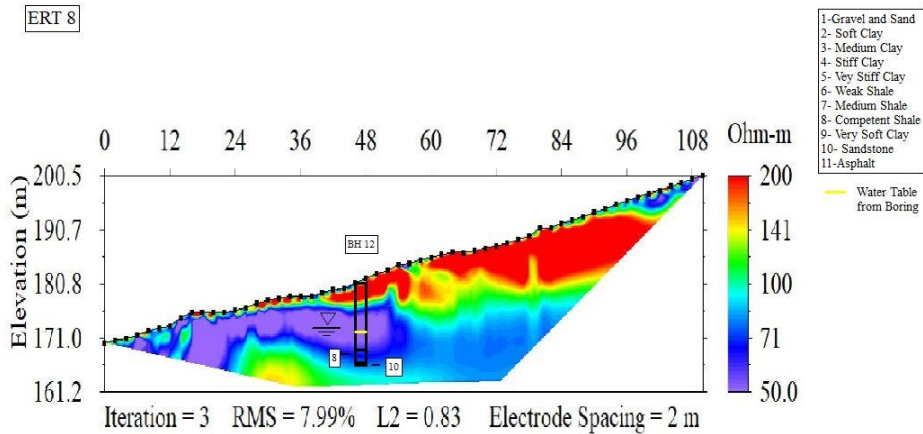




(a)



(b)



(c)

Figure 23- Ozark Site (a) ERT Line 1, (b) ERT Line 3, (c) ERT Line 8 (Used with Permission from West Koehn)

It should be noted that the resistivity of shale is very similar to that of water, and therefore at the Ozark site the conclusions drawn from the ERT data relied heavily on the borings. With that in mind, Figure 23 was interpreted as follows:

- The purple layers in ERT 1 agree with the water tables reported in the borings. It also suggests that there is potential that the top of the light blue line represents soil saturated above the water table due to capillary rise. Therefore, the soils along ERT 1 may be saturated closer to the surface than originally believed. A phreatic surface was used in the model; however, so the water table was kept as the location of interest.
- ERT 3 suggests that saturated soils may be encountered at lower elevations on the east side of the site opposed to the west side, but this should be considered with caution. Where this zone is showing higher water presence is also located near the edge of the inverted data and it could be a function of this feature as opposed to actual changes in the moisture conditions.
- The rise in elevation of the green and yellow coloring in the bottom left corner of ERT 8 suggests that there may be a rise in the bedrock just north, (i.e., downhill) of BH 12. A similar signature was also seen in the seismic geophysical data.

Data was also collected from MASW lines conducted across the site. MASW 1 was compared to BH 6, BH 10, BH 13, BH 16, and BH 18, MASW 3 was compared to BH 4, BH 8, and BH 12 and MASW 8 was compared to BH 12. Figure 24 shows the MASW lines with boring log overlays for MASW 1, MASW 3, and MASW 8.

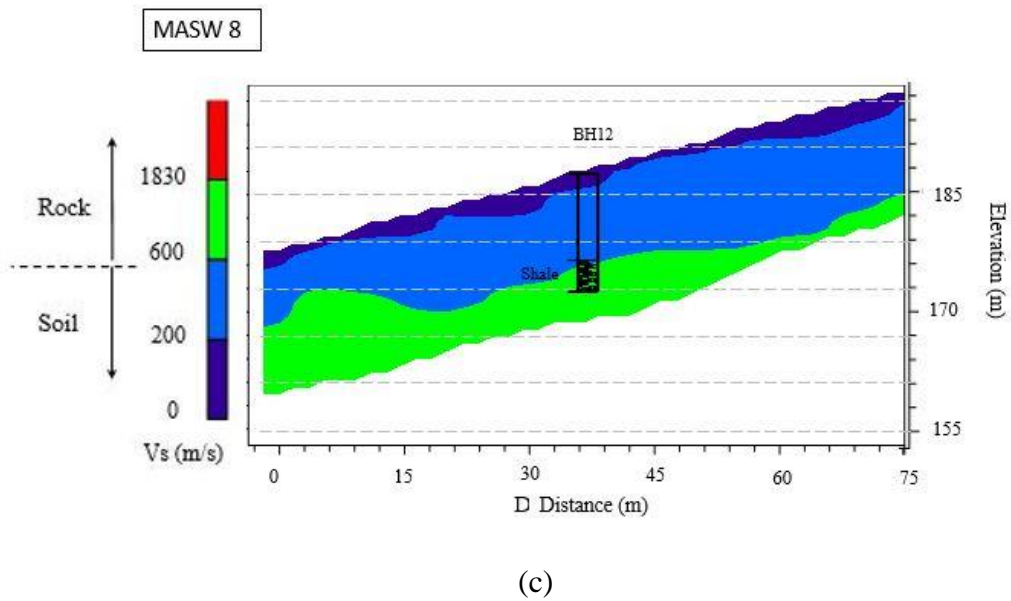
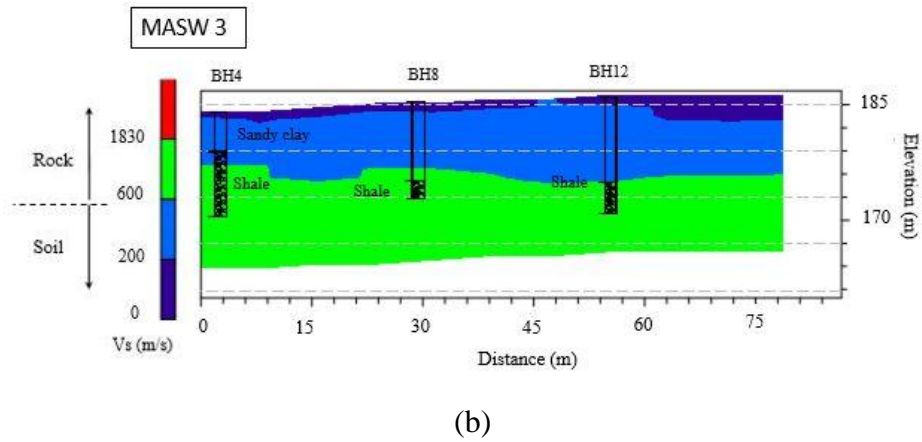
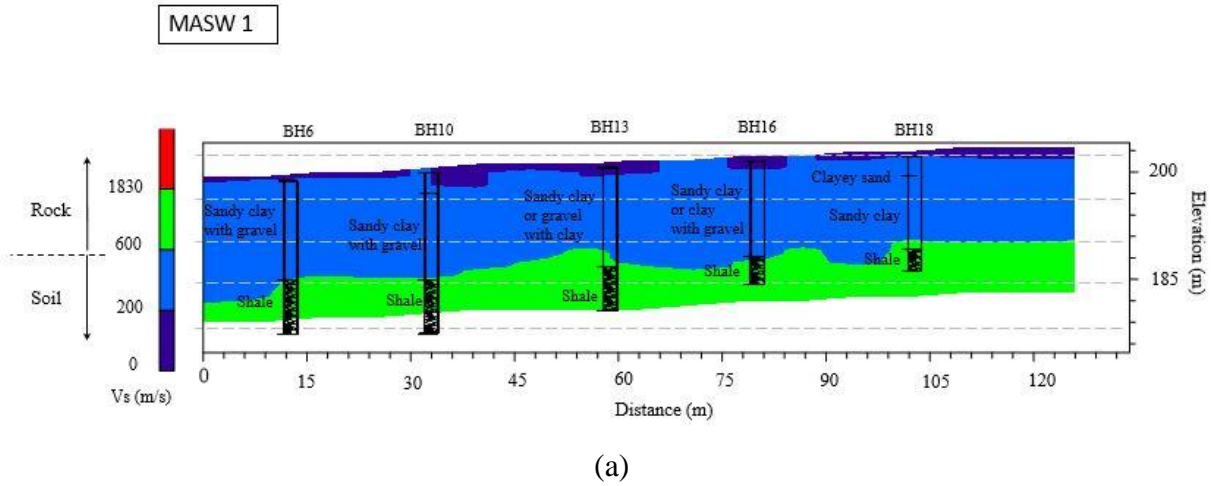
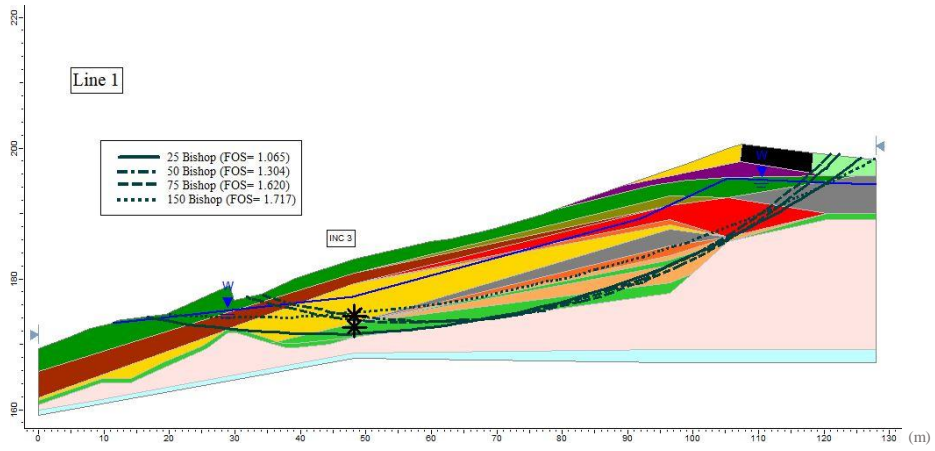


Figure 24- Ozark Site (a) MASW Line 1, (b) MASW Line 3, (c) MASW Line 8 (Used with Permission from Salman Rahimi)

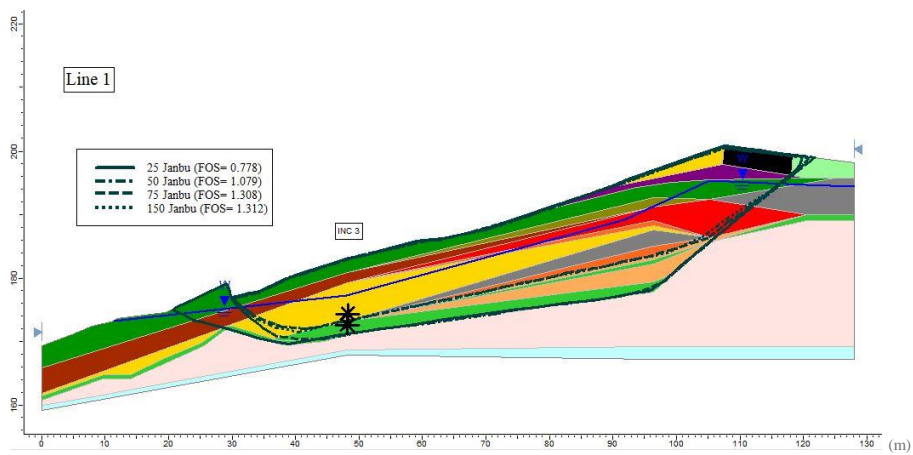
The following interpretations can be made from Figure 24:

- The green shale layers from MASW 1 and MASW 3 intersect the borings in different parts of the shale layers (weak, medium, and competent.) and therefore, it should be noted that the MASW data may not be able to distinguish between different degrees of weathering observed in the boring logs. In most of the locations where boring logs could be directly compared, there was a layer of weather material sitting on top of more competent material. This was not distinguishable in the MASW and HVSR data, but it was considered in the modeling.
- MASW 8 also suggests that there is a bump up in the bedrock north of BH 12, which confirms the speculation made from the ERT data. This is likely a physical feature that should be included in the models.

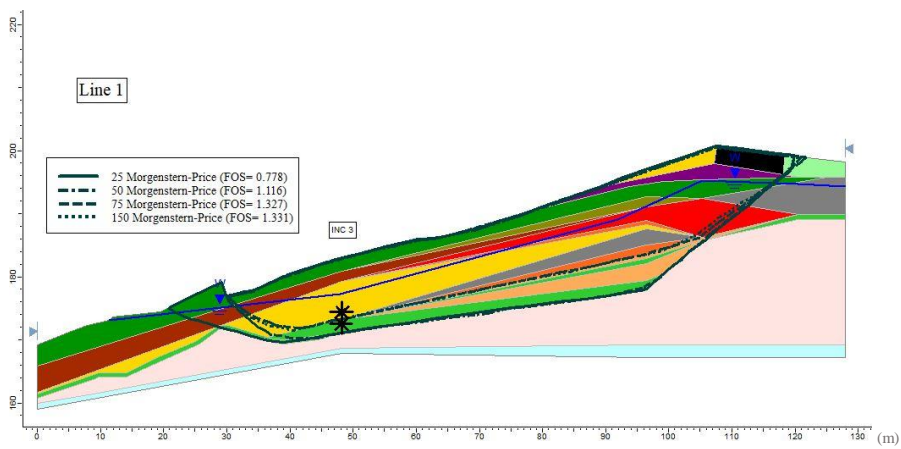
The main adjustments made from the Phase 1 to Phase 2 models was raising the phreatic surface to and adding the bedrock bump located just north, downhill, of BH 12. It should be noted that a thin (0.6 m) layer of weathered shale was carried along the top of the bedrock to account for a likely present weathered seam. Figure 25 shows the models for Line 1 Phase 2 for each of the methods. The inclinometer slip zone from Inclinometer 3 is denoted by black asterisks.



(a)



(b)

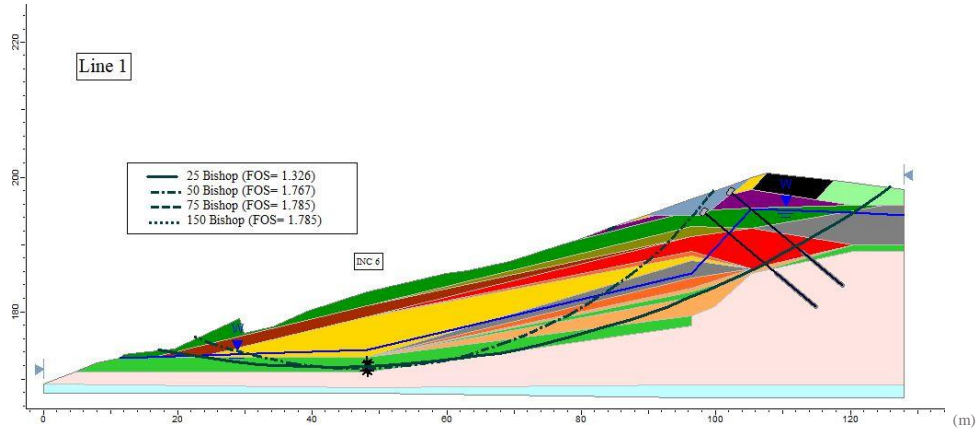


(c)

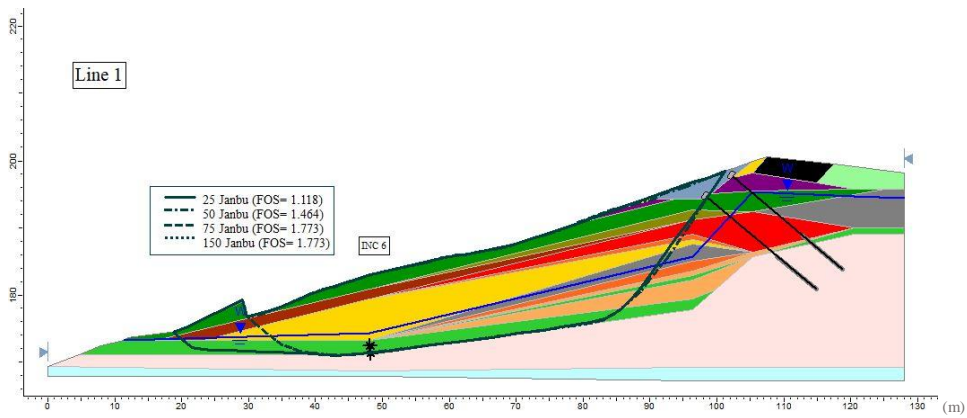
Figure 25- Parametric Study for Phase 2 Line 1 using (a) Simplified Bishop, (b) Simplified Janbu, (c) Morgenstern-Price Method

The failure surfaces displayed in Figure 25 are very similar to that of Figure 24 for each scenario, with the exception of a few minor shifts due to the bedrock rise at the toe. Additionally, the FOSs changed on average less than 2% from Phase 1 to Phase 2, with the exception of the 25 kPa slip surface for Simplified Bishop which increased by 11% from Phase 1 to Phase 2. Figure 24 and Figure 25 show that the addition of geophysical data only have minor effects on the failure surfaces and FOSs for Line 1 before anchor installation.

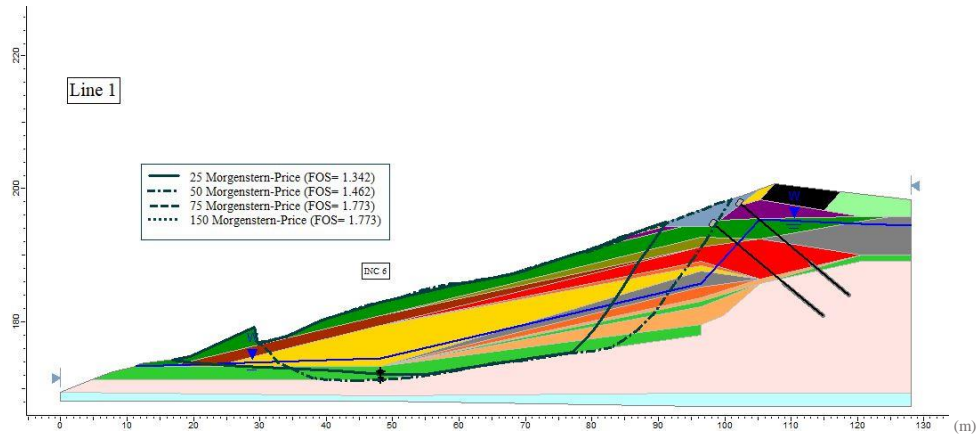
Phase 3 considers the analysis of the slope after the anchors were installed using only data collected from the borings. For Line 1, two rows of anchors were installed. It should be noted that soil was excavated, the anchors were installed, and then fill material was placed back on top of the anchors. Inclinator 6 was used to compare the model slip surfaces, as it was closest to Line 1 and was installed after the anchors. The slide zone from the inclinometer is denoted by black asterisks. Figure 26 shows Phase 3 results for all methods for Line 1.



(a)



(b)



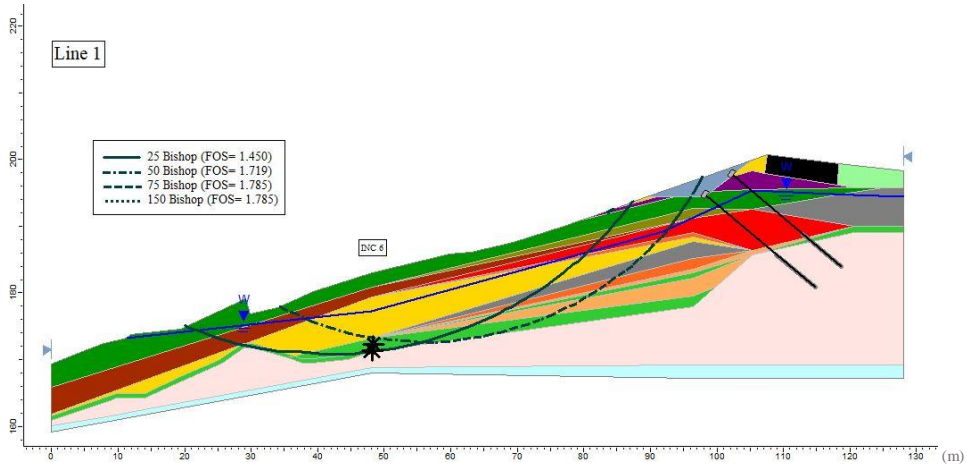
(c)

Figure 26- Parametric Study for Phase 3 Line 1 using (a) Simplified Bishop, (b) Simplified Janbu, (c) Morgenstern-Price Method

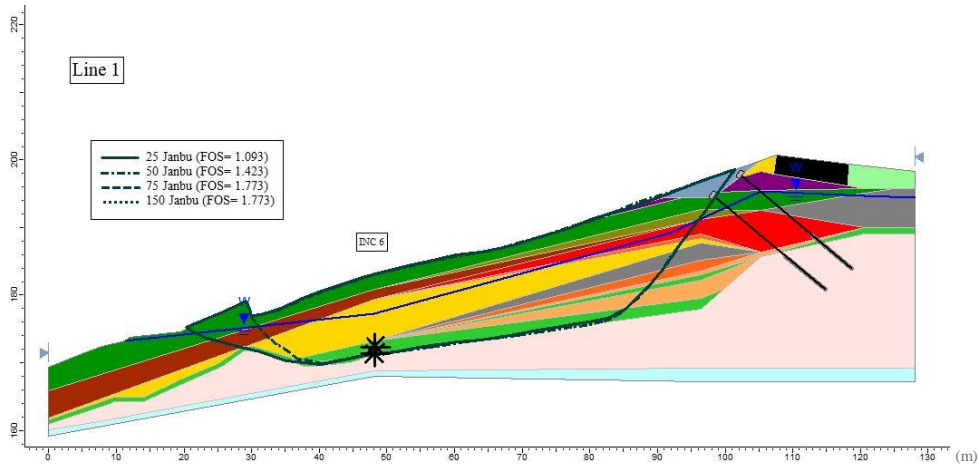
The addition of the anchors shifted the top of the slip surface from the south, uphill, side of the road to the north, downhill, side of the road for all methods except the Simplified Bishop method where the weak layer had a strength of 25 kPa. Additionally, all of the scenarios where the weak layer had a strength of 75 kPa or 150 kPa, the failure becomes a small, shallow surface failure. The FOSs all increased and are all greater than 1.3, the acceptable design FOS, with the exception of the 25 kPa scenario using Simplified Janbu method. Therefore, depending on the analysis method used and the accepted strength value used for the weak layer, the anchors could appear as an acceptable fix for this particular section of the slope when using boring log information only.

Phase 4 Part 1 includes the geophysical data in addition to the boring data for Line 1 after anchor installation. The same changes based on geophysical data were made for Phase 4 that were implemented in Phase 2.

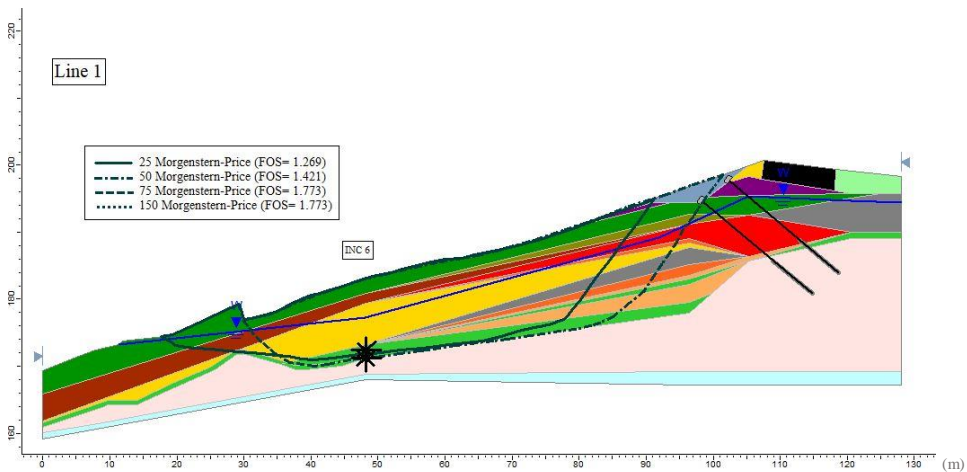




(a)



(b)

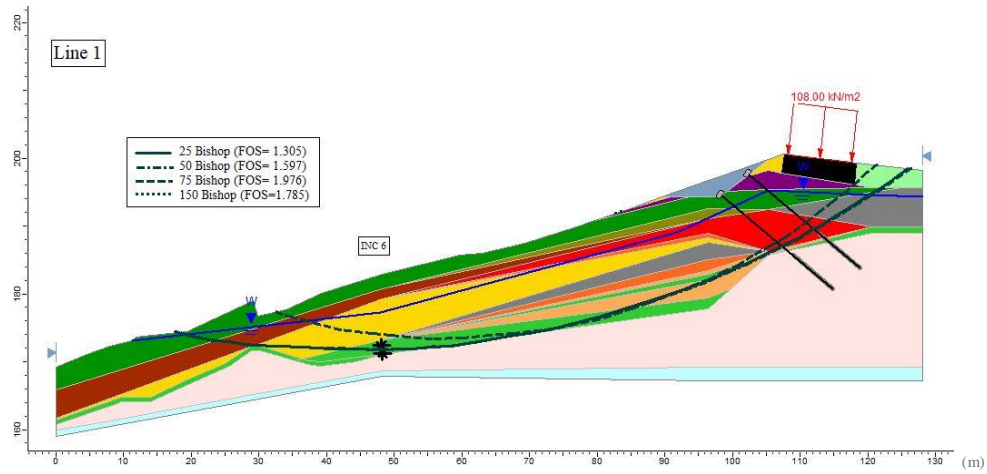


(c)

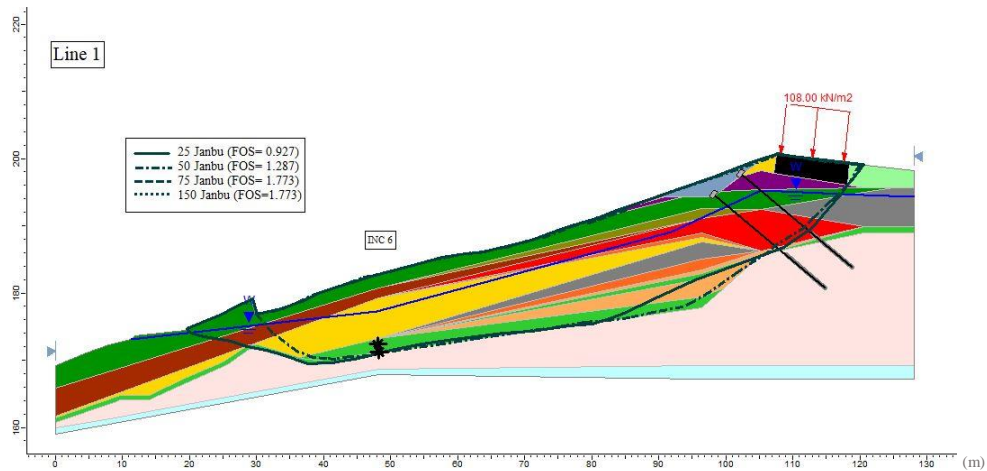
Figure 27- Parametric Study for Phase 4 Part 1 Line 1 using (a) Simplified Bishop, (b) Simplified Janbu, (c) Morgenstern-Price Method

The addition of geophysical data changed the failure locations for Simplified Bishop methods, but had little effect on the failure surfaces in the Simplified Janbu and Morgenstern-Price methods. The three FOSs most affected by the addition of the geophysical data were Simplified Bishop 25 kPa, Simplified Janbu 75 kPa, and Morgenstern-Price 75 kPa where the FOSs increased by 9.4%, 21.2% and 21.3%, respectively. The other FOSs either were not impacted or decreased by 5.4% or less. This indicates that the addition of geophysics could have a significant impact on FOS on Line 1 after anchor installation depending on the analysis method and soil strength values used. For the weakest strength used, the FOS for Janbu and Morgenstern-Price decreased slightly and was below the 1.3 value typically seen as a safe design.

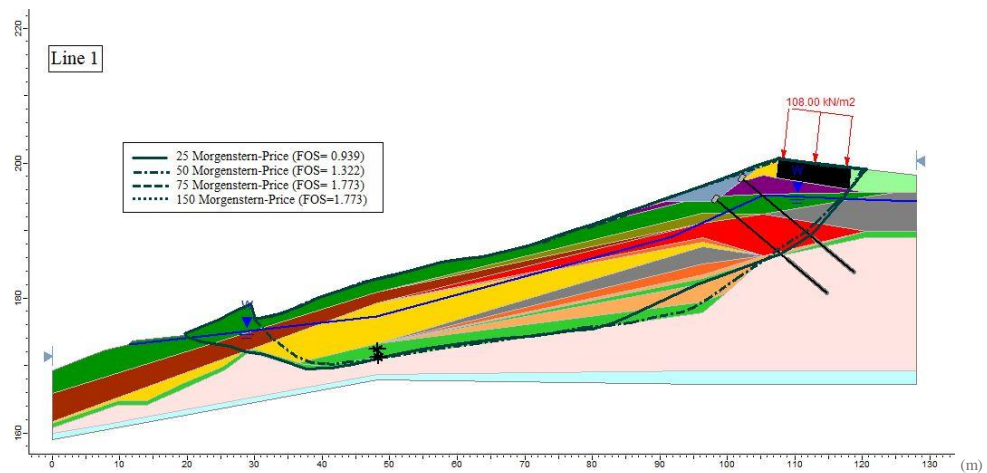
The last phase for Line 1 is Phase 4 Part 2 which is the same as Phase 4 Part 1, but a traffic load of 108 kPa is added to the roadway. Similar to the Sand Gap Site, this particular interstate is a fairly heavily trucked road. Figure 28 shows the results from Phase 4 Part 2 for all methods.



(a)



(b)



(c)

Figure 28- Parametric Study for Phase 4 Part 2 Line 1 using (a) Simplified Bishop, (b) Simplified Janbu, (c) Morgenstern-Price Method

After the addition of a traffic load, the failure surfaces for weak layer strength values of 25 kPa and 50 kPa changed for all methods. The FOSs for the 25 kPa scenario change by 10%, 15.2%, and 26% for Simplified Bishop, Simplified Janbu, and Morgenstern-Price, respectively. The FOS for each method for the 50 kPa scenario changed between 7-10%. Phase 4 Part 2 suggests that the addition of traffic loading can significantly impact the anticipated FOS. It should be noted that if the weak layer has a strength value of 25 kPa or less, the Simplified Janbu and Morgenstern-Price methods have a FOS less than 1.0 for this scenario suggesting a failure would happen even after anchors have been installed. Table 11 shows all of the FOSs for each of the phases for Line 1.

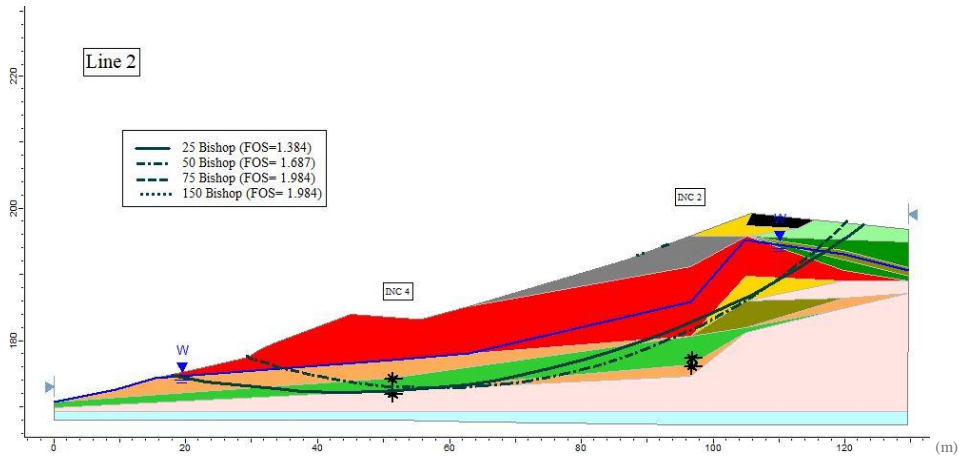
Table 11: FOS Tabulations for Ozark Site Line 1

<b>Line 1 Phase 1</b>	<b>Weak Layer Strength (kPa)</b>	<b>Simplified Bishop</b>	<b>Simplified Janbu</b>	<b>Morgenstern-Price</b>
	<b>25</b>	0.959	0.763	0.769
	<b>50</b>	1.277	1.066	1.105
	<b>75</b>	1.591	1.33	1.357
	<b>150</b>	1.772	1.312	1.337
<b>Line 1 Phase 2</b>	<b>Weak Layer Strength (kPa)</b>	<b>Simplified Bishop</b>	<b>Simplified Janbu</b>	<b>Morgenstern-Price</b>
	<b>25</b>	1.065	0.778	0.778
	<b>50</b>	1.304	1.079	1.116
	<b>75</b>	1.62	1.308	1.327
	<b>150</b>	1.717	1.312	1.331
<b>Line 1 Phase 3</b>	<b>Weak Layer Strength (kPa)</b>	<b>Simplified Bishop</b>	<b>Simplified Janbu</b>	<b>Morgenstern-Price</b>
	<b>25</b>	1.326	1.111	1.342
	<b>50</b>	1.767	1.464	1.462
	<b>75</b>	1.785	1.464	1.462
	<b>150</b>	1.785	1.773	1.773
<b>Line 1 Phase 4 Part 1 (without Traffic Load)</b>	<b>Weak Layer Strength (kPa)</b>	<b>Simplified Bishop</b>	<b>Simplified Janbu</b>	<b>Morgenstern-Price</b>
	<b>25</b>	1.45	1.093	1.269
	<b>50</b>	1.719	1.423	1.421
	<b>75</b>	1.785	1.773	1.773
	<b>150</b>	1.785	1.773	1.773
<b>Line 1 Phase 4 Part 2 (with Traffic Load)</b>	<b>Weak Layer Strength (kPa)</b>	<b>Simplified Bishop</b>	<b>Simplified Janbu</b>	<b>Morgenstern-Price</b>
	<b>25</b>	1.305	0.927	0.939
	<b>50</b>	1.597	1.287	1.322
	<b>75</b>	1.976	1.773	1.773
	<b>150</b>	1.785	1.773	1.773

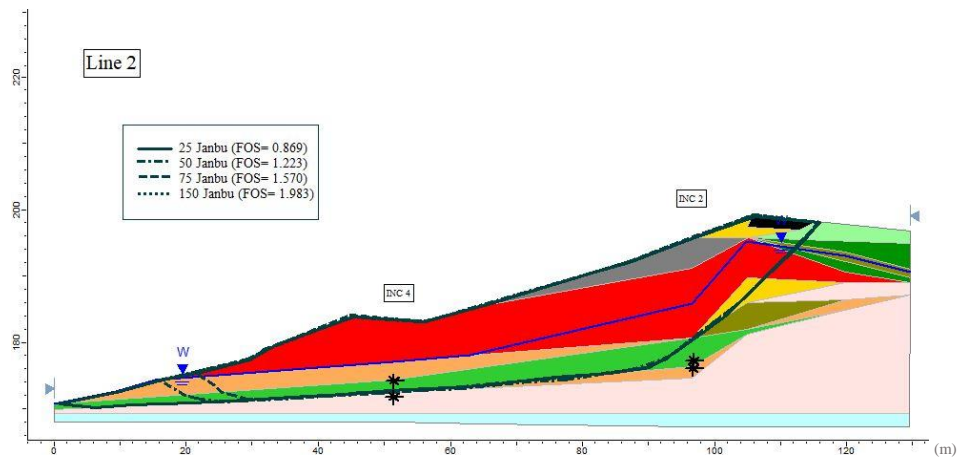
## *Line 2*

Figure 29 shows the Phase 1, borings only, model for Line 2. Line 2, like Line 1, contains many different soil layers across the slope, but the important layers are the weak layer (light green), medium shale layer (light orange), and competent shale layer (light pink). Similar to Line 1, parametric studies were carried out to examine the effects of various strength values for the weak layer. Data from Inclinator 2 and Inclinator 4 were used for Line 2 before the

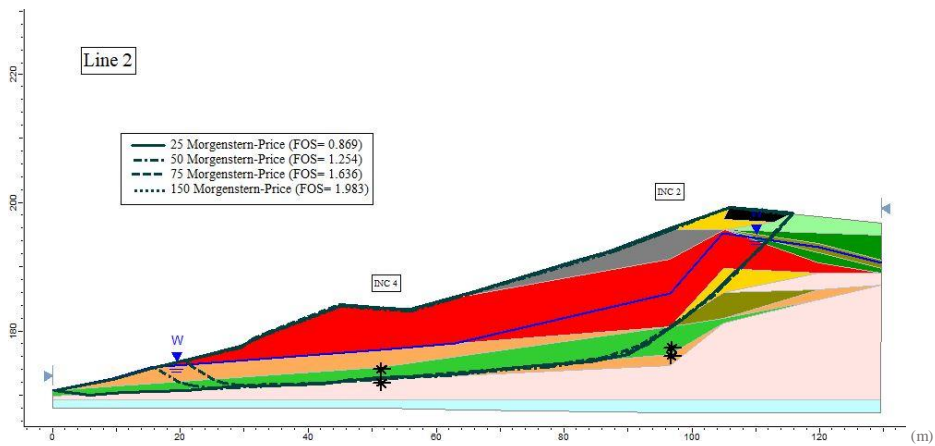
anchors were installed. It should be noted that the line does not directly cut through the inclinometer locations and therefore, the slide zones may be different than suggested in Figure 29. The inclinometer slip zone is indicated by black asterisks.



(a)



(b)



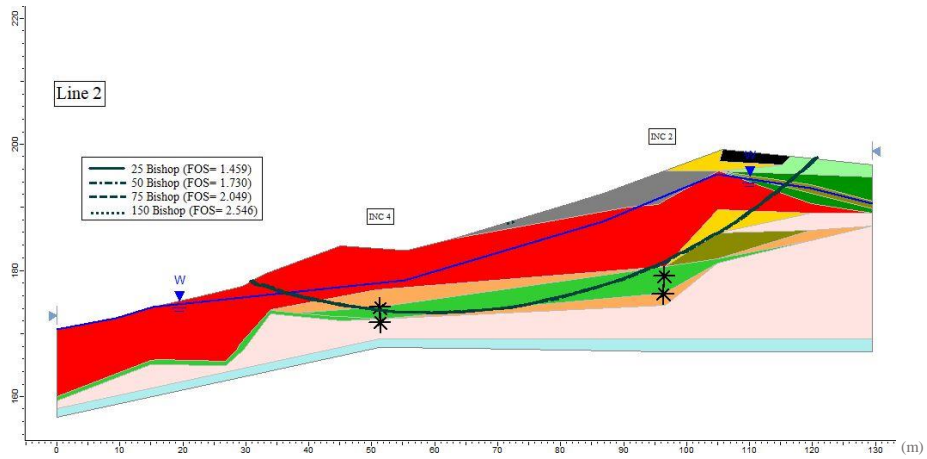
(c)

Figure 29- Parametric Study for Phase 1 Line 2 using (a) Simplified Bishop, (b) Simplified Janbu, (c) Morgenstern-Price Method

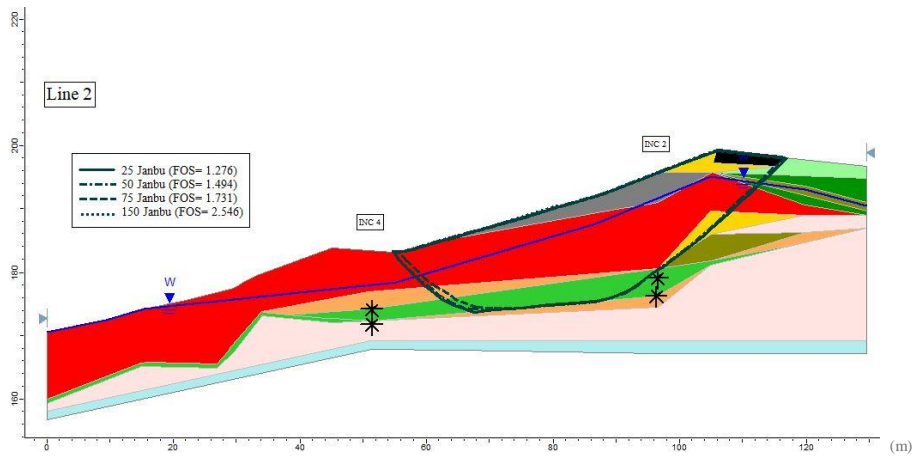
The parametric study for Line 2 shows that when the weak layer strength value is 150 kPa the failure is a shallow surface failure for all methods. This agrees with the earlier models that suggest that the weak layer may be weaker than the boring data suggests. It should also be noted, that for Line 2 based on borings only, if the weak layer undrained shear strength value is 25 kPa or less, than the slope will likely fail. Additionally, all methods for 25 kPa and 50 kPa show the slip lining up with data from Inclinator 4, but differing from Inclinator 2. This could again be in part due to Line 2 not cutting exactly through Inclinator 2.

Phase 2 for Line 2 includes data from the MASW, HVSR, and ERT data. Similar to Line 1 Phase 2, the phreatic surface was raised, and a bedrock rise was added toward the bottom of the slope, located just north of BH 8. Figure 30 shows the results for Line 2 Phase 2.

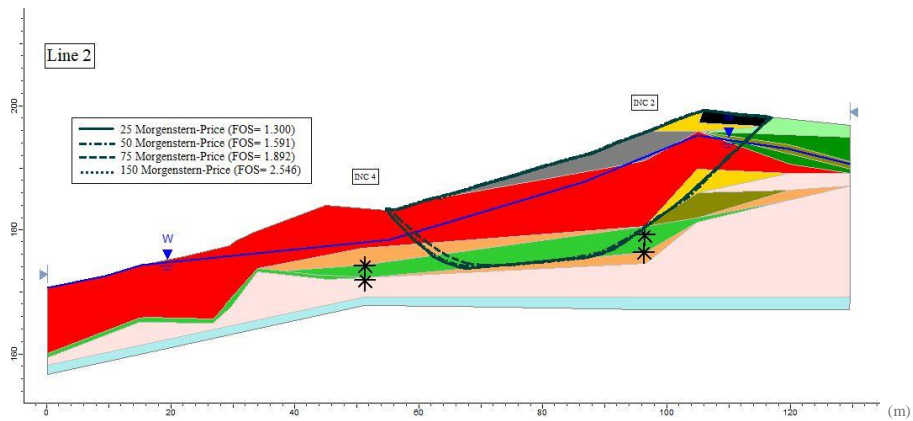




(a)



(b)

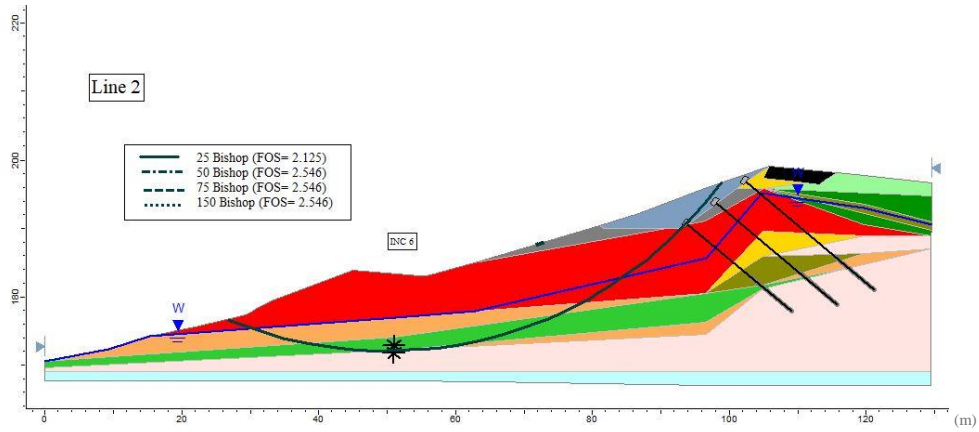


(c)

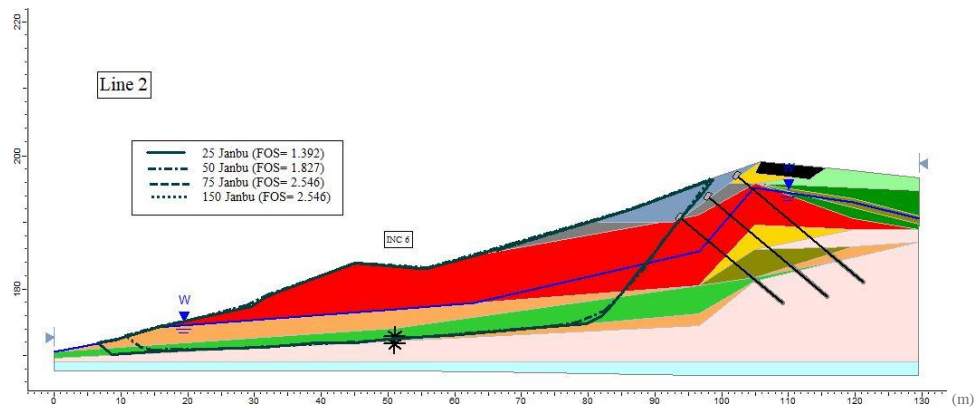
Figure 30- Parametric Study for Phase 2 Line 2 using (a) Simplified Bishop, (b) Simplified Janbu, (c) Morgenstern-Price Method

The addition of the geophysics raised the FOSs for all of the methods. All of the FOSs are above 1.0 suggesting that the slope is no longer failing and they are all above the accepted design FOS of 1.3 with the exception of the Simplified Janbu method for 25 kPa which has a FOS of 1.276 which almost meets the criteria. Additionally, the slip surfaces changed fairly drastically for the Simplified Janbu and Morgenstern-Price methods. The toe of the failure traveled south up the slope and the failure surfaces no longer go through the slip zone indicated by Inclinator 4.

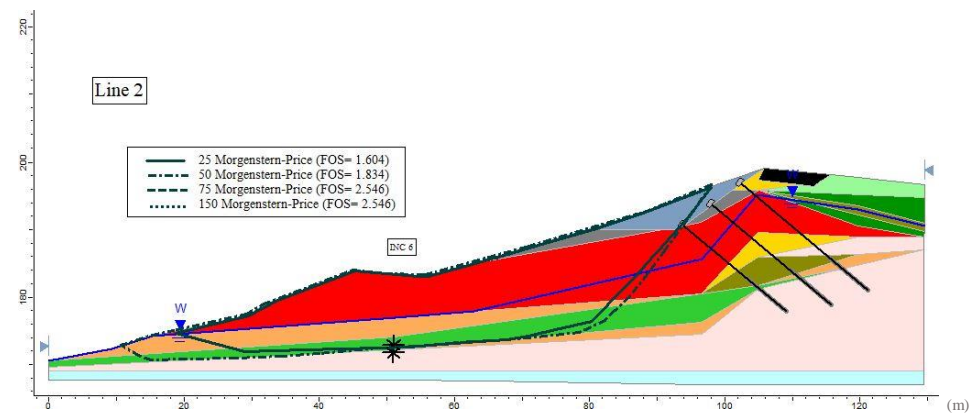
Phase 3 uses data from borings only and models the slope after anchors were installed. Line 2 was located in an area where three anchors were installed. These anchors were also covered by fill following installation. Figure 31 shows the analyses for Line 2 Phase 3. It should be noted that Inclinator 6 was used once anchors were installed and is located in BH 8 directly where Line 2 cuts through the Ozark site.



(a)



(b)



(c)

Figure 31- Parametric Study for Phase 3 Line 2 using (a) Simplified Bishop, (b) Simplified Janbu, (c) Morgenstern-Price Method

The installation of three anchors for Line 2 shifted all of the slip surfaces to downslope of the road, north of the anchors. Additionally, all of the FOSs are above 1.3 which indicate an acceptably designed slope after anchor installation.

Phase 4 Part 1 for Line 2 includes geophysical data in addition to the boring data and is modeling the slope after anchor installation. The same adjustments based on geophysical data were made for Phase 4 that were made for Phase 2. Figure 32 shows the results from the slope analyses for Line 2 Phase 4 Part 1.

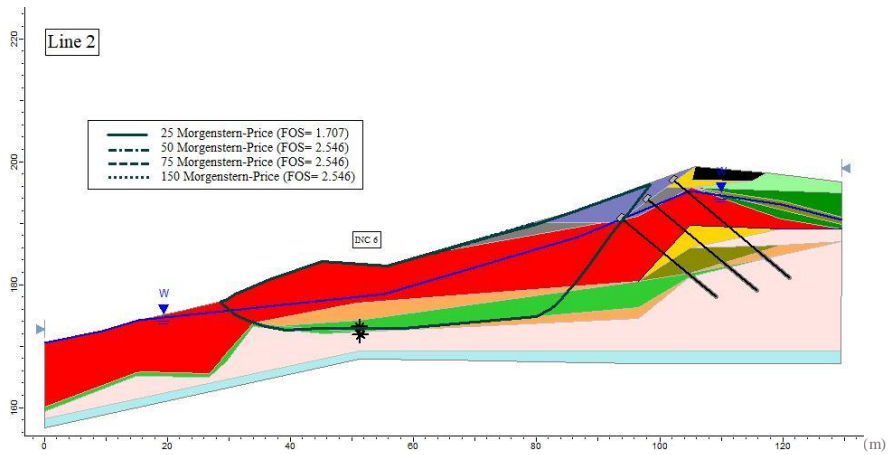
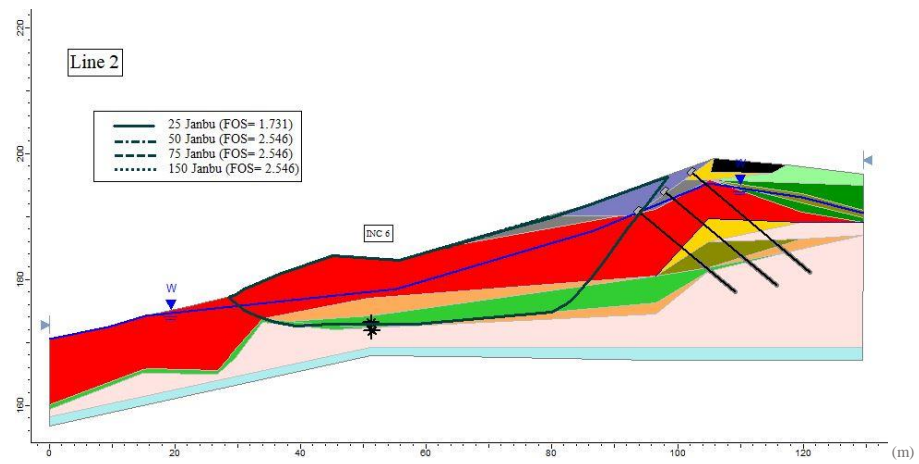
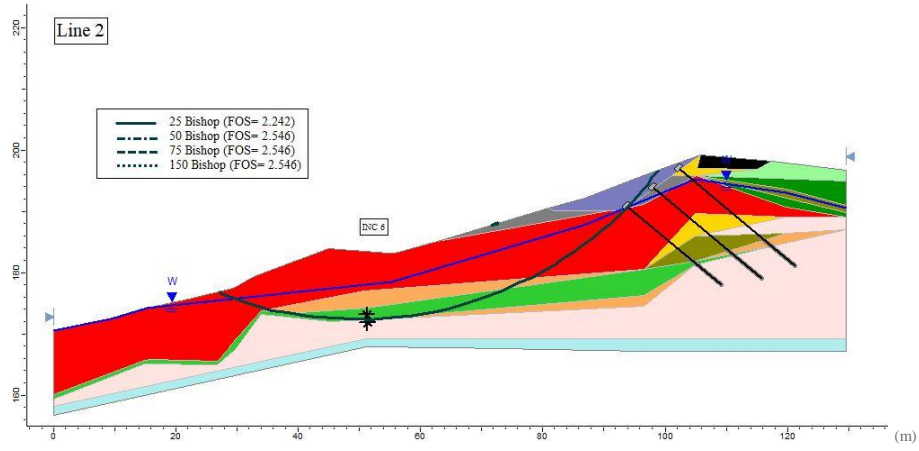
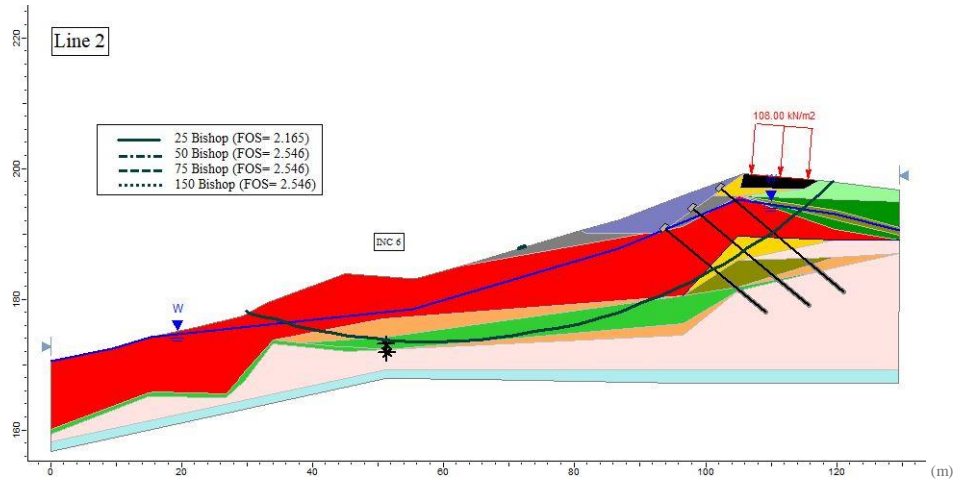


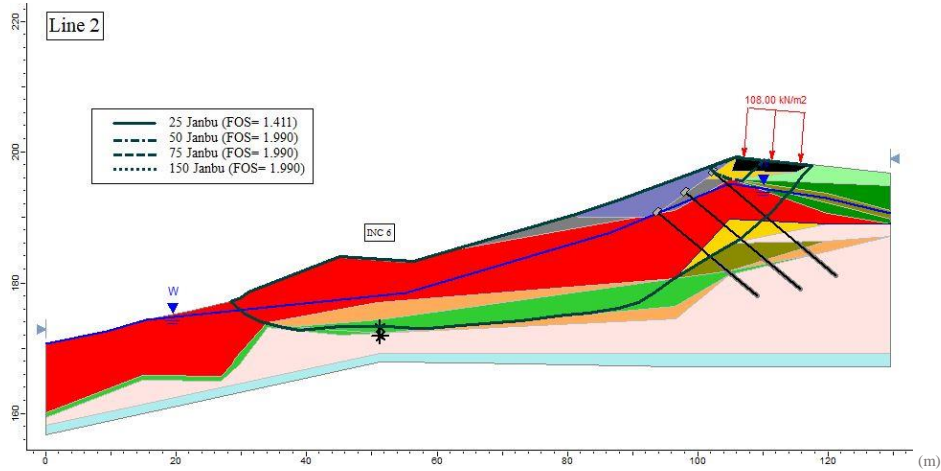
Figure 32- Parametric Study for Phase 4 Part 1 Line 2 using (a) Simplified Bishop, (b) Simplified Janbu, (c) Morgenstern-Price Method

The addition of geophysical data increased the FOSs even more making it where all FOSs are greater than 1.7, which is far above the necessary fact FOS for design. Additionally, when the weak layer is presumed to have a strength of 50 kPa the failure has become a shallow surface failure for all methods. Based on the addition of geophysical data, Line 2 after anchor installation is not going to fail.

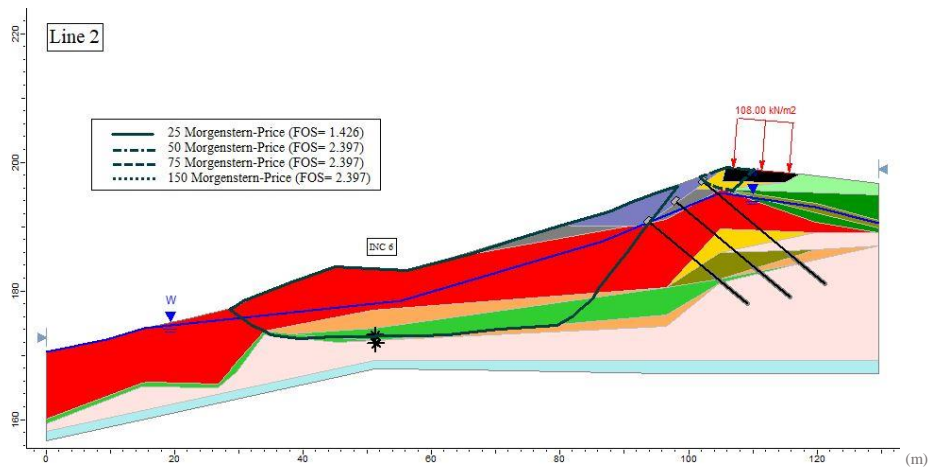
The final phase, Phase 4 Part 2, for Line 2 is exactly like Phase 4 Part 1 only a traffic load of 108 kPa was added to the road way. Figure 33 shows the slope analyses for Line 2 Phase 4 Part 2.



(a)



(b)



(c)

Figure 33- Parametric Study for Phase 4 Part 2 Line 2 using (a) Simplified Bishop, (b) Simplified Janbu, (c) Morgenstern-Price Method

The slip surfaces for the 25 kPa scenario for the Simplified Bishop and Simplified Janbu methods change and include the roadway in the failure. The Morgenstern-Price method for the 25 kPa scenario remains unchanged from Phase 4 Part 1. Additionally, the failure surfaces for the 50 kPa, 75 kPa, and 150 kPa scenarios for the Simplified Janbu and Morgenstern-Price methods also changed location. They are now small failures located immediately north of the roadway. Lastly, it should be noted that some of the FOSs lowered, but still remained above 1.3 for all scenarios indicating that even when traffic loads are considered, three rows of anchors appear to be an appropriate mitigation strategy. Table 12 shows all of the FOSs for each of the phases for Line 2.



Table 12: FOS Tabulations for Ozark Site Line 2

<b>Line 2 Phase 1</b>	<b>Weak Layer Strength (kPa)</b>	<b>Simplified Bishop</b>	<b>Simplified Janbu</b>	<b>Morgenstern-Price</b>
	<b>25</b>	1.384	0.869	0.869
	<b>50</b>	1.687	1.223	1.254
	<b>75</b>	1.984	1.57	1.636
	<b>150</b>	1.984	1.983	1.983
<b>Line 2 Phase 2</b>	<b>Weak Layer Strength (kPa)</b>	<b>Simplified Bishop</b>	<b>Simplified Janbu</b>	<b>Morgenstern-Price</b>
	<b>25</b>	1.459	1.276	1.300
	<b>50</b>	1.730	1.494	1.591
	<b>75</b>	2.049	1.731	1.892
	<b>150</b>	2.546	2.546	2.546
<b>Line 2 Phase 3</b>	<b>Weak Layer Strength (kPa)</b>	<b>Simplified Bishop</b>	<b>Simplified Janbu</b>	<b>Morgenstern-Price</b>
	<b>25</b>	2.125	1.392	1.604
	<b>50</b>	2.546	1.827	1.834
	<b>75</b>	2.546	2.546	2.546
	<b>150</b>	2.546	2.546	2.546
<b>Line 2 Phase 4 Part 1 (without Traffic Load)</b>	<b>Weak Layer Strength (kPa)</b>	<b>Simplified Bishop</b>	<b>Simplified Janbu</b>	<b>Morgenstern-Price</b>
	<b>25</b>	2.242	1.731	1.707
	<b>50</b>	2.546	2.546	2.546
	<b>75</b>	2.546	2.546	2.546
	<b>150</b>	2.546	2.546	2.546
<b>Line 2 Phase 4 Part 2 (with Traffic Load)</b>	<b>Weak Layer Strength (kPa)</b>	<b>Simplified Bishop</b>	<b>Simplified Janbu</b>	<b>Morgenstern-Price</b>
	<b>25</b>	2.165	1.411	1.426
	<b>50</b>	2.546	1.990	2.397
	<b>75</b>	2.546	1.990	2.397
	<b>150</b>	2.546	1.990	2.397

### Conclusion

Slope stability analyses were conducted for two slopes in Arkansas. Models were generated using traditional geotechnical boring log data and compared to models generated using boring log data and geophysical data. From this study the following conclusions can be drawn:

- Based on inclinometer data and the slope model analyses one of the main factors that contributed to the slope failures at the Sand Gap and Ozark site was the presence of a weathered, weak bedrock layer at the interface of the soil and bedrock
- When combined with borings, ERT, MASW, and HVSr data can be useful tools to determine the presence of water and locate bedrock across a site. It should be noted, however, that these methods cannot easily distinguish between thin weathered layers above bedrock and unweathered bedrock, which is an important feature needed in a slope stability analysis.
- In areas where boring information is limited, the use of geophysics can inform the slope stability analysis and impact the slip surface location and FOS. Boring log data, although discrete, provides much more information about the soil conditions and only small improvements in the analysis were observed when geophysical data was added to an already extensive drilling and sampling program.
- The addition of a traffic load can significantly affect the FOS and slip location, and therefore should be considered when designing a slope on a heavily trucked road

Additionally, when doing a slope stability analysis it is imperative to have key information about the slope including accurate relative elevations, soil layer depths and thicknesses, water content, methods to obtain soil strength values (sampling, SPT, and CPT correlations), full awareness of any bedrock weathering, and samples of weathered bedrock so that strength values can be obtained.

## References

Albataineh, N. (2006) "Slope Stability Analysis using 2D and 3D methods," thesis for the degree Master of Science, University of Akron, pp 1-36.

Bishop, A. W. (1955). The use of the slip circle in the stability analysis of slopes. *Géotechnique*, 5(1), 7-17.

*Data acquisition*. Retrieved October 9, 2018, from <http://www.masw.com/DataAcquisition.html>

Duncan, M.J. & Wright, S.G. (2005). *Soil strength and slope stability*. New Jersey: John Wiley and Sons, INC.

EEGS. *What is geophysics?* Retrieved October 17, 2018, from <https://www.eegs.org/what-is-geophysics->

Everett, M. (2014). *Near-Surface Applied Geophysics*. Cambridge: Cambridge University Press. doi:10.1017/CBO9781139088435

Google. (n.d.). [Google Earth location of Sand Gap, Arkansas]. Retrieved May 4, 2019, from <https://www.google.com/earth/>

Google. (n.d.). [Google Earth location of Ozark, Arkansas]. Retrieved May 4, 2019, from <https://www.google.com/earth/>

Janbu, N. (1973). "Slope Stability Computations," *Embankment Dam Engineering - Casagrande Volume*, John Wiley and Sons, N.Y.

Janbu, N., Bjerrum, L., and Kjaernsli, B.: (1956), "Soil mechanics applied to some engineering problems", Norwegian Geotechnical Institute, Publication 16, pp. 5-26.

Jongmans, D., & Garambois, S. (2007). Geophysical investigation of landslides : A review. *Bulletin De La Societe Geologique De France*, 178(2), 101-112.

- Júnior, L. S. B., Prado, R. L., & Mendes, R. M. (2012). Application of multichannel analysis of surface waves method (masw) in an area susceptible to landslide at ubatuba city, brazil. *Revista Brasileira De Geofísica*, 30(2)
- Lane, J., White, E., Steele, G., & Cannia, J. (2008). *Estimation of bedrock depth using the horizontal-to-vertical (H/V) ambient-noise seismic method*
- Leshchinsky, B.A., & Ambauen, S. (2015). Limit Equilibrium and Limit Analysis: Comparison of Benchmark Slope Stability Problems.
- Lin, H., Zhong, W., Xiong, W., & Tang, W. (2014). Slope stability analysis using limit equilibrium method in nonlinear criterion. *TheScientificWorldJournal*, 2014, 206062. (Retraction published ScientificWorldJournal. 2015)
- Matthews, C.R., Farook, Z., & Helm, P.J. (2014). Slope stability analysis - limit equilibrium or the finite element method?
- Meyerhof, G. G. (1956). Penetration tests and bearing capacity of cohesionless soils. *Journal of the Soil Mechanics and Foundation Division*, 82(1), 1-19.
- Morgenstern, N.R. and Price, V.E. (1965) The Analysis of the Stability of General Slip Surfaces. *Géotechnique*, 15, 79-93.
- Moudabel, O. A. M. (2013). Slope stability case study by limit equilibrium and numerical methods. ProQuest Dissertations Publishing). Retrieved from Dissertations & Theses Europe Full Text: Science & Technology database. Retrieved from <https://search.proquest.com/docview/1426246867>
- Park, C. B., & Miller, R. D. (2008). Roadside passive multichannel analysis of surface waves (MASW). *Journal of Environmental & Engineering Geophysics*, 13(1), 1-11.
- Pasierb, B., Grodecki, M., & Gwózdź, R. (2019). Geophysical and geotechnical approach to a landslide stability assessment: A case study. *Acta Geophysica*,

- Pazzi, V., Tanteri, L., Bicocchi, G., D'Ambrosio, M., Caselli, A., & Fanti, R. (2016). H/V measurements as an effective tool for the reliable detection of landslide slip surfaces: Case studies of castagnola (la spezia, italy) and roccalbegna (grosseto, italy). *Physics and Chemistry of the Earth*, 98, 136-153.
- Pazzi, V., Morelli, S., & Fanti, R. (2019). A review of the advantages and limitations of geophysical investigations in landslide studies. *International Journal of Geophysics*, 2019, 1-27.
- Pourkhosravani, A., Kalantari, B. (2011). *A review of current methods for slope stability evaluation. Electronic Journal of Geotechnical Engineering*, 16
- Race, M. L., & Coffman, R. A. Effect of uncertainty in site characterization on the prediction of liquefaction potential for bridge embankments in the mississippi embayment. *Geo-congress 2013* (pp. 888-897)
- Schuster, R. L. (1996). *Landslides: Investigation and Mitigation. Chapter 2- Socioeconomic Significance of Landslides (No. 247)*
- Sowers, G. B., & Sowers, G. F. (1970). *Introductory soil mechanics and foundations*. New York: MacMillan Publishing.
- Stark, T. D., & Ruffing, D. G. Selecting minimum factors of safety for 3D slope stability analyses. *Geo-risk 2017* (pp. 259-266)
- Tosatti, G. (2008). Slope instability processes affecting the pietra di bismantova geosite (northern apennines, italy). *Geoheritage*, 2(3), 155-168
- USGS. *How Many Deaths Result From Landslides Each Year?* Retrieved from [https://www.usgs.gov/faqs/how-many-deaths-result-landslides-each-year?qt-news\\_science\\_products=3#qt-news\\_science\\_products](https://www.usgs.gov/faqs/how-many-deaths-result-landslides-each-year?qt-news_science_products=3#qt-news_science_products)
- Wines, D.. (2016). A comparison of slope stability analyses in two and three dimensions. *Journal of the Southern African Institute of Mining and Metallurgy*, 116(5), 399-406. <https://dx.doi.org/10.17159/2411-9717/2016/v116n5a5>

Wright, Stephen G., Fred H. Kulhawy, and James M. Duncan. (1973) "Accuracy of Equilibrium Slope Stability Analysis," *Journal of the Soil Mechanics and Foundations Division*, ASCE, Vol. 99, No. pp. 783-791

Zhou, Bing ED1 - Ali, Ismet Kanl. (2019). Electrical resistivity tomography: A subsurface imaging technique. *Applied geophysics with case studies on environmental, exploration and engineering geophysics* (pp. Ch. 7). Rijeka: IntechOpen.